NOAA NESDIS
CENTER for SATELLITE APPLICATIONS and RESEARCH

ALGORITHM THEORETICAL BASIS DOCUMENT

ABI Cloud Height

Andrew Heidinger, NOAA/NESDIS/STAR

Version 3.0

July 2012

TABLE OF CONTENTS

1 INTRODUCTION ... 9
  1.1 Purpose of This Document ... 9
  1.2 Who Should Use This Document ... 9
  1.3 Inside Each Section ... 9
  1.4 Related Documents ... 9
  1.5 Revision History ... 9
2 OBSERVING SYSTEM OVERVIEW ... 12
  2.1 Products Generated ... 12
  2.2 Instrument Characteristics ... 17
3 ALGORITHM DESCRIPTION ... 19
  3.1 Algorithm Overview ... 19
  3.2 Processing Outline ... 19
  3.3 Algorithm Input ... 21
    3.3.1 Primary Sensor Data ... 21
    3.3.2 Ancillary Data ... 21
    3.3.3 Derived Data ... 22
  3.4 Theoretical Description ... 24
    3.4.1 Physics of the Problem ... 24
      3.4.1.1 Motivation for ACHA Channel Selection ... 24
      3.4.1.2 Radiative Transfer Equation ... 28
      3.4.1.3 Cloud Microphysical Assumptions ... 29
    3.4.2 Mathematical Description ... 32
      3.4.2.1 Estimation of Prior Values and their Uncertainty ... 35
      3.4.2.2 Estimation of Forward Model Uncertainty ... 36
      3.4.2.3 Estimation of Quality Flags and Errors ... 37
      3.4.2.4 Impact of Local Radiative Center Pixels ... 37
      3.4.2.5 Treatment of Multi-layer Clouds ... 38
      3.4.2.6 Pixel Processing Order with the ACHA ... 39
      3.4.2.7 Computation of Cloud Height and Cloud Pressure ... 39
      3.4.2.8 Computation of Cloud Layer ... 41
    3.4.3 Algorithm Output ... 41
      3.4.3.1 Output ... 41
      3.4.3.2 Intermediate data ... 42
      3.4.3.3 Product Quality Flag ... 42
      3.4.3.4 Processing Information Flag ... 42
      3.4.3.5 Metadata ... 43
4 Test Datasets and Outputs ... 44
  4.1 Simulated/Proxy Input Datasets ... 44
    4.1.1 SEVIRI Data ... 45
      4.1.1.1 CALIPSO Data ... 46
  4.2 Output from Simulated/Proxy Inputs Datasets ... 46
    4.2.1 Precisions and Accuracy Estimates ... 52
      4.2.1.1 MODIS Analysis ... 52
        4.2.1.1.1 Comparison of Cloud-top Pressure ... 54

4.2.1.1.2 Comparison of Cloud-top Temperature ... 55
4.2.1.2 CALIPSO Analysis ... 56
4.2.1.2.1 Validation of Cloud Top Height ... 57
4.2.1.2.2 Validation of Cloud Top Temperature ... 60
4.2.1.2.3 Validation of Cloud Top Pressure ... 61
4.2.1.2.4 Validation of Cloud Layer ... 61
4.2.2 Error Budget ... 63
5 PRACTICAL CONSIDERATIONS ... 64
5.1 Numerical Computation Considerations ... 64
5.2 Programming and Procedural Considerations ... 64
5.3 Quality Assessment and Diagnostics ... 64
5.4 Exception Handling ... 64
5.5 Algorithm Validation ... 64
6 ASSUMPTIONS AND LIMITATIONS ... 64
6.1 Performance ... 65
6.2 Assumed Sensor Performance ... 65
6.3 Pre-Planned Product Improvements ... 65
6.3.1 Optimization for Atmospheric Motion Vectors ... 65
6.3.2 Implementation of Channel Bias Corrections ... 65
6.3.3 Use of 10.4 μm Channel ... 66
7 REFERENCES ... 67
Appendix 1: Common Ancillary Data Sets ... 69
1. NWP_GFS ... 69
a. *Data description* ... 69
b. Interpolation description ... 69
2. SFC_ELEV_GLOBE_1KM ... 70
a. *Data description* ... 70
b. *Interpolation description* ... 70
3. SFC_TYPE_AVHRR_1KM ... 71
a. *Data description* ... 71
b. *Interpolation description* ... 71
4. LRC ... 71
a. Data *description* ... 71
b. Interpolation *description* ... 71
5. CRTM ... 76
a. Data *description* ... 76
b. Interpolation *description* ... 76
c. CRTM calling procedure in the AIT framework ... 77

LIST OF FIGURES

Figure 1 High level flowchart of the ACHA illustrating the main processing sections. . 20
Figure 2 A false color image constructed from 11 – 12μm BTD (Red), 4 – 11μm BTD (Green) and 11 μm BT reversed (Blue). Data are taken from AQUA/MODIS and CALIPSO/CALIOP on August 10, 2006 from 20:35 to 20:40 UTC. The red line is the CALIPSO track. In this color combination, cirrus clouds appear white but as the optical thickness increases, the ice clouds appear as light blue/cyan. Low-level water clouds appear as dark blue, and mid-level water clouds tend to have a red/orange color. 25
Figure 3 The 532 nm total backscatter from CALIOP along the red line shown in Figure 2. The grey line in the centre image is the Tropopause. 26
Figure 4 Cloud-top pressure solution space provided by the ACHA channel set for the ice clouds along the CALIPSO track for August 10, 2006 20:35 – 20:40 UTC. The grey lines represent the solution space provided by the selected GOES-R ABI channels. The black symbols provide the CALIOP cloud boundaries for the highest cloud layer. The blue points represent the location of the optimal cloud-top pressure solutions with this channel set. For clarity, only every fifth optimal cloud-top pressure solution is plotted. 27
Figure 5 Same as Figure 4 computed for the VIIRS channel set (3.75, 8.5, 11 and 12 μm). Red points show the MODIS (MYD06) results for reference. 27
Figure 6 Comparison of the variation of β values for 11 and 12 μm against those for 12 and 8.5 μm. The cloud of points represents those computed using CALIPSO observations collocated with MODIS. The lines represent predictions based on the Yang et. al scattering database. 30
Figure 7 Computed variation and linear-fit of the 11 and 13.3 μm β values to those computed using 11 and 12 μm. β is a fundamental measure of the spectral variation of cloud emissivity, and this curve is used in the forward model in the retrieval. The data shown are for ice crystals with an aggregate habit. For water clouds, Mie theory predicts a = -0.217 and b = 1.250. 31
Figure 8 Variation of the 11 and 12 μm β values as a function of the ice crystal radius. This relation is used in the retrieval to produce an estimate of cloud particle size from the final retrieved β values... 32
Figure 9 Schematic illustration of multi-layer clouds.. 39
Figure 10 Illustration of a cloud located in a temperature inversion. (Figure provided by Bob Holz of UW/SSEC). 41
Figure 11 Full disk 0.63, 0.86 and 11 μm false color image from SEVIRI for 12 UTC on January 17, 2006. 45
Figure 12 Illustration of CALIPSO data used in this study. Top image shows a 2D backscatter profile. Bottom image shows the detected cloud layers overlaid onto the backscatter image. Cloud layers are colored magenta. (Image courtesy of Michael Pavolonis, NOAA) 46
Figure 13 Example ACHA output of cloud-top temperature derived from SEVIRI proxy data for January 17, 2006. 47
Figure 14 Example ACHA output of cloud-top pressure derived from SEVIRI proxy data for January 17, 2006. 48
Figure 15 Example ACHA output of cloud-top height derived from SEVIRI proxy data for January 17, 2006. 49

Figure 16 Example ACHA output of cloud-top layer derived from SEVIRI proxy data for January 17, 2006. 50
Figure 17 Example ACHA output of the 11μm cloud emissivity derived from SEVIRI proxy data for January 17, 2006 51
Figure 18 Example images illustrating a comparison of MODIS and SEVIRI data. Image at the top right shows the MODIS 0.65 μm reflectance. Top left image shows the SEVIRI 0.65 μm reflectance. Bottom left image shows the time difference in minutes. Bottom right image shows the pixels used in the analysis. Black colored regions were excluded based on differences in the MODIS and SEVIRI 0.65 μm reflectance and 11 μm brightness temperature. Red, green and blue colored pixels were used in the analysis. 53
Figure 19 Comparison of cloud-top pressure for June 13, 2008 at 12:15 UTC over Western Europe derived from the MODIS (MYD06) products and from the Cloud Application Team's baseline approach applied to SEVIRI data. Bias (accuracy) and the standard deviation (precision) of the comparison are shown in the figure. 54
Figure 20 Comparison of cloud-top temperature for June 13, 2008 at 12:15 UTC over Western Europe derived from the MODIS (MYD06) products and from the Cloud Application Team's baseline approach applied to SEVIRI data. Bias (accuracy) and the standard deviation (precision) of the comparison are shown in the figure. 55
Figure 21 Distribution of points used in the validation of the ACHA applied to SEVIRI data for data observed during simultaneous SEVIRI and CALIPSO periods over eight weeks from four seasons in 2006 and 2007. 57
Figure 22 Distribution of cloud-top height mean bias (accuracy) as a function of cloud height and cloud emissivity as derived from CALIPSO data for all SEVIRI observations for four two-week periods covering all seasons. Bias is defined as ACHA – CALIPSO. 58
Figure 23 Distribution of cloud-top height of the standard deviation of the bias (precision) as a function of cloud height and cloud emissivity as derived from CALIPSO data for all SEVIRI for four two-week periods covering all seasons. Bias is defined as ACHA – CALIPSO.......... 59
Figure 24 Distribution of cloud-top temperature mean bias (accuracy as a function of cloud height and cloud emissivity as derived from CALIPSO data for all SEVIRI observations for four two-week periods covering all seasons. Bias is defined as ACHA – CALIPSO. 60
Figure 25 Distribution of cloud-top temperature of the standard deviation of the bias (precision) as a function of cloud height and cloud emissivity as derived from CALIPSO data for all SEVIRI observations for four two-week periods covering all seasons. Bias is defined as ACHA – CALIPSO. 61

LIST OF TABLES

Table 1. Requirements from F&PS version 2.2 for Clear sky Mask 16
Table 2. Channel numbers and wavelengths for the ABI (*- planned, but requires additional research from the GOES-RRR program.) 17
Table 3: The a priori (first guess) retrieval values used in the ACHA retrieval. 36
Table 4: Values of uncertainty for the forward model used in the ACHA retrieval. 37
Table 5. Channel numbers and wavelengths for the ABI (*- planned, but requires additional research from the GOES-RRR program.) 44
Table 6. Preliminary estimate of error budget for ACHA. 63

LIST OF ACRONYMS

1DVAR - one-dimensional variational
ABI - Advanced Baseline Imager
AIT - Algorithm Integration Team
ATBD - algorithm theoretical basis document
A-Train – Afternoon Train (Aqua, CALIPSO, CloudSat, etc.)
AVHRR - Advanced Very High Resolution Radiometer
AWG - Algorithm Working Group
BT – Brightness Temperature
BTD – Brightness Temperature Difference
CALIPSO - Cloud-Aerosol Lidar and Infrared Pathfinder Satellite
CIMSS - Cooperative Institute for Meteorological Satellite Studies
CLAVR-x - Clouds from the Advanced Very High Resolution Radiometer (AVHRR) Extended
CRTM - Community Radiative Transfer Model (CRTM), currently under development.
ECWMF - European Centre for Medium-Range Weather Forecasts
EOS - Earth Observing System
EUMETSAT- European Organization for the Exploitation of Meteorological Satellites
F&PS - Function and Performance Specification
GFS - Global Forecast System
GOES - Geostationary Operational Environmental Satellite
GOES-RRR – GOES-R Risk Reduction
IR – Infrared
IRW – IR Window
ISCCP – International Satellite Cloud Climatology Project
MODIS - Moderate Resolution Imaging Spectroradiometer
MSG - Meteosat Second Generation
NASA - National Aeronautics and Space Administration
NESDIS - National Environmental Satellite, Data, and Information Service
NOAA - National Oceanic and Atmospheric Administration
NWP - Numerical Weather Prediction
PFAAST - Pressure layer Fast Algorithm for Atmospheric Transmittances
PLOD - Pressure Layer Optical Dept
POES - Polar Orbiting Environmental Satellite
RTM - radiative transfer model
SEVIRI - Spinning Enhanced Visible and Infrared Imager
SSEC – Space Science and Engineering Center
STAR - Center for Satellite Applications and Research
VIIRS – Visible Infrared Imager Radiometer Suite
UW – University of Wisconsin at Madison

ABSTRACT

This document describes the algorithm for GOES-R ABI Cloud Height Algorithm (ACHA). The ACHA generates the cloud-top height, cloud-top temperature, cloud-top pressure and cloud layer products. The ACHA uses only infrared observations in order to provide products that are consistent for day, night and terminator conditions. The ACHA uses analytical model of infrared radiative transfer imbedded into an optimal estimation retrieval methodology. Cloud-top pressure and cloud-top height are derived the cloud-top temperature product and the atmospheric temperature profile provided by Numerical Weather Prediction (NWP) data. Cloud layer is derived solely from the cloud-top pressure product.

The ACHA uses the spectral information provided by the GOES-R ABI to derive cloud-top height information simultaneously with cloud microphysical information. Currently, the ACHA employs the 11, 12 and 13.3 μm observations. This information allows the ACHA to avoid making assumptions on cloud microphysics in the retrieval of cloud height. As a consequence, ACHA also generates the intermediate products of 11 μm cloud emissivity and an 11/12 μm microphysical index.

This document will describe the required inputs, the theoretical foundation of the algorithms, the sources and magnitudes of the errors involved, practical considerations for implementation, and the assumptions and limitations associated with the product, as well as provide a high level description of the physical basis for estimating height of tops of clouds observed by the ABI. The results from running the ACHA on SEVIRI, which served as a proxy for ABI, validated against the CALIOP LIDAR as well as a comparison to the MODIS Cloud height product are also shown.

INTRODUCTION

1.1 Purpose of This Document

The primary purpose of this ATBD is to establish guidelines for producing the cloud-top height, cloud-top temperature and cloud-top pressure from the ABI flown on the GOES-R series of NOAA geostationary meteorological satellites. This document will describe the required inputs, the theoretical foundation of the algorithms, the sources and magnitudes of the errors involved, practical considerations for implementation, and the assumptions and limitations associated with the product, as well as provide a high level description of the physical basis for estimating height of tops of clouds observed by the ABI. Unless otherwise stated, the determination of cloud-top height always implies the simultaneous determination of temperature and pressure. The cloud-top height is made available to all subsequent algorithms which require knowledge of the vertical extent of the clouds. The cloud-top height also plays a critical role in determining the cloud cover and layers product.

1.2 Who Should Use This Document

The intended users of this document are those interested in understanding the physical basis of the algorithms and how to use the output of this algorithm to optimize the cloud height output for a particular application. This document also provides information useful to anyone maintaining or modifying the original algorithm.

1.3 Inside Each Section

This document is broken down into the following main sections:

- **System Overview**: provides relevant details of the ABI and provides a brief description of the products generated by the algorithm.
- **Algorithm Description**: provides a detailed description of the algorithm including its physical basis, its input and its output.
- **Assumptions and Limitations**: provides an overview of the current limitations of the approach and notes plans for overcoming these limitations with further algorithm development.

1.4 Related Documents

This document currently does not relate to any other document outside of the specifications of the GOES-R F&PS and to the references given throughout.

1.5 Revision History

Version 2.0 of this document was created by Dr. Andrew Heidinger of NOAA/NESDIS and its intent was to accompany the delivery of the version 4 algorithm to the GOES-R AWG AIT. This document was then revised following the document guidelines provided by the GOES-R Algorithm Application Group (AWG) before the version 0.5 delivery.

Version 1.0 of the document includes some new results from the algorithm Critical Design Review (CDR) and the Test Readiness Review (TRR), as well as the algorithm 80% readiness document.

OBSERVING SYSTEM OVERVIEW
This section describes the products generated by the ABI Cloud Height Algorithm (ACHA) and its associated sensor requirements.

1.6 Products Generated

The ACHA is responsible for estimation of vertical extent for all cloudy ABI pixels. In terms of the F&PS, it is responsible directly for the Cloud-Top Pressure, Height and Temperature products. The cloud height is also used to generate a cloud-layer flag which classifies a cloud as being a high, middle or low-level cloud. This flag is used in generating the cloud-cover layers product. The ACHA results are currently used in the daytime and nighttime cloud optical and microphysical algorithms. In addition, cloud-top pressure results from this algorithm are expected to be used in the Atmospheric Motion Vector (AMV) algorithm.

In addition to the cloud height metrics (pressure/temperature/height), the ACHA also provides an estimate of the 11 μm cloud emissivity and a microphysical parameter, β, derived from multiple emissivities that are related to particle size. These products, as described later, are generated automatically by the ACHA and are useful for evaluating the ACHA's performance. The requirements for the ACHA from the F&PS version 2.2 are stated below in Table 1, with height, pressure, temperature, layer from top to bottom for each geographic coverage.

Table 1. Requirements from F&PS version 2.2.

Cloud Top Height Requirements

Name	**Geographic Coverage (G, H, C, M)**	**Vertical Resolution**	**Horizontal Resolution**	**Mapping Accuracy**	**Measurement Range**	**Measurement Accuracy**	**Refresh Rate/Coverage Time (Mode 3)**	**Refresh Rate/Coverage**	**Vendor-Allocated Ground Latency**	**Vendor-Allocated Ground Latency (Mode 4)**	**Product Measurement Precision**
Cloud Top Height	C	Cloud Top	10 km	5 km	100 – 300 km	500 m for clouds with emissivity > 0.8	60 min	60 min	266 sec	266 sec	1500 m for clouds with emissivity > 0.8
Cloud Top Height	FD	Cloud Top	10 km	5 km	0 – 15 km	500 m for clouds with emissivity > 0.8	60 min	60 min	806 sec	806 sec	1500 m for clouds with emissivity > 0.8

Cloud Top Height	M	Cloud Top	4 km	2 km	0 – 20 km	500 m for clouds with emissivity > 0.8	5 min		266 sec		1500 m for clouds with emissivity > 0.8

Cloud Top Height Product Qualifiers

Name	User & Priority	Geographic Coverage (G, H, C, M)	Temporal Coverage Qualifiers	Product Extent Qualifier	Cloud Cover Conditions Qualifier	Product Statistics Qualifier
Cloud Top Height	GOES-R	C	Day and night	Quantitative out to at least 62 degrees LZA and qualitative at larger LZA	Clear conditions associated with threshold accuracy	Over specified geographic area
Cloud Top Height	GOES-R	FD	Day and night	Quantitative out to at least 62 degrees LZA and qualitative at larger LZA	Clear conditions associated with threshold accuracy	Over specified geographic area
Cloud Top Height	GOES-R	M	Day and night	Quantitative out to at least 62 degrees LZA and qualitative at larger LZA	Clear conditions associated with threshold accuracy	Over specified geographic area

Cloud Top Pressure Requirements

Name	Geographic Coverage	Vertical Resolution	Horizontal Resolution	Mapping Accuracy	Measurement Range	Measurement Accuracy	Refresh Rate/Coverage Time (Mode 3)	Refresh Rate/Coverage Time (Mode 3)	Vendor-Allocated Ground Latency (Mode 3)	Vendor-Allocated Ground Latency	Product Measurement Precision
Cloud Top Pressure	C	Cloud Top	10 km	5 km	100 – 1000 mb	50 mb for clouds with emissivity > 0.8	60 min	60 min	536 sec	536 sec	150 mb for clouds with emissivity > 0.8
Cloud Top Pressure	FD	Cloud Top	10 km	5 km	100 – 1000 mb	50 mb for clouds with emissivity > 0.8	60 min	60 min	806 sec	806 sec	150 mb for clouds with emissivity > 0.8

Cloud Top Pressure Product Qualifiers

Name	User & Priority	Geographic Coverage (G, H, C, M)	Temporal Coverage Qualifiers	Product Extent Qualifier	Cloud Cover Conditions Qualifier	Product Statistics Qualifier
Cloud Top Pressure	GOES-R	C	Day and night	Quantitative out to at least 62 degrees LZA and qualitative at larger LZA	Clear conditions associated with threshold accuracy	Over specified geographic area
Cloud Top Pressure	GOES-R	FD	Day and night	Quantitative out to at least 62 degrees LZA and qualitative at larger LZA	Clear conditions associated with threshold accuracy	Over specified geographic area

Cloud Top Temperature Requirements

Name	Geographic Coverage	Vertical Resolution	Horizontal Resolution	Mapping Accuracy	Measurement Range	Measurement Accuracy	Refresh Rate/Coverage Time (Mode 3)	Refresh Rate/Coverage Time (Mode 4)	Vendor-Allocated Ground Latency (Mode 3)	Vendor-Allocated Ground Latency (Mode 4)	Product Measurement Precision
Cloud Top Temperature	FD	At Cloud Tops	2 km	1 km	180 – 300 K	3 K for clouds with emissivity > 0.8	15 min	15 min	806 sec	806 sec	5 K for clouds with emissivity > 0.8
Cloud Top Temperature	M	At Cloud Tops	2 km	1 km	180 – 300 K	3 K for clouds with emissivity > 0.8	5 min		266 sec		5 K for clouds with emissivity > 0.8

Cloud Top Temperature Product Qualifiers

Name	User & Priority	Geographic Coverage (G, H, C, M)	Temporal Coverage Qualifiers	Product Extent Qualifier	Cloud Cover Conditions Qualifier	Product Statistics Qualifier
Cloud Top Temperature	GOES-R	FD	Day and night	Quantitative out to at least 65 degrees LZA and qualitative at larger LZA	In presence of clouds with optical depth >1. Clear conditions down to cloud top associated with threshold accuracy	Over specified geographic area
Cloud Top Temperature	GOES-R	M	Day and night	Quantitative out to at least 65 degrees LZA and qualitative at larger LZA	In presence of clouds with optical depth >1. Clear conditions down to cloud top associated with threshold accuracy	Over specified geographic area

Cloud Layers/Heights Requirements

Name	Geographic Coverage (G, H, C, M)	Vertical Resolution	Horizontal Resolution	Mapping Accuracy	Measurement Range	Measurement Accuracy	Refresh Rate/Coverage Time (Mode 3)	Refresh Rate/Coverage Time (Mode 4)	Vendor-Allocated Ground Latency (Mode 3)	Product Measurement Precision
Cloud Layers/ Heights	C	1 cloud layer	10 km	5 km	Low, Mid, High	80% correct classification	60 min	5 min	806 sec	1 category
Cloud Layers/ Heights	FD	1 cloud layer	10 km	5 km	Low, Mid, High	80% correct classification	60 min	5 min	806 sec	1 category
Cloud Layers/ Heights	M	1 cloud layer	4 km	2 km	Low, Mid, High	80% correct classification	5 min		266 sec	1 category

Cloud Layers/Heights Product Qualifiers

Name	User & Priority	Geographic Coverage	Temporal Coverage Qualifiers	Product Extent Qualifier	Cloud Cover Conditions Qualifier	Product Statistics Qualifier
Cloud Layers/ Heights &Thickness	GOES-R	C	Day and night	Quantitative out to at least 62 degrees LZA and qualitative at larger LZA	In presence of clouds with optical depth >1. Clear conditions down to cloud top associated with threshold accuracy	Over specified geographic area

Cloud Layers/ Heights &Thickness	GOES-R	FD	Day and night	Quantitative out to at least 62 degrees LZA and qualitative at larger LZA	In presence of clouds with optical depth >1. Clear conditions down to cloud top associated with threshold accuracy	Over specified geographic area
Cloud Layers/ Heights &Thickness	GOES-R	M	Day and night	Quantitative out to at least 62 degrees LZA and qualitative at larger LZA	In presence of clouds with optical depth >1. Clear conditions down to cloud top associated with threshold accuracy	Over specified geographic area

Furthermore, the GOES-R Series Ground Segment (GS) Project Functional and Performance Specification (F&PS) qualifies these requirements for cloudy regions with emissivities greater than 0.8 .

1.7 Instrument Characteristics

The ACHA will operate on each pixel determined to be cloudy or probably cloud by the ABI Cloud Mask (ACM). . Table 2 summarizes the current channels used by the ACHA.

Table 2. Channel numbers and wavelengths for the ABI Cloud Height Algorithm (ACHA)

Channel Number	*Wavelength (μm)*	*Used in ACHA*
1	0.47	
2	0.64	
3	0.86	
4	1.38	
5	1.61	
6	2.26	
7	3.9	
8	6.15	
9	7.0	
10	7.4	
11	8.5	
12	9.7	
13	10.35	

14	11.2	✓
15	12.3	✓
16	13.3	✓

In general, the ACHA relies on the infrared observations to avoid discontinuities associated with the transition from day to night. ACHA performance is sensitive to imagery artifacts or instrument noise. Most important is our ability to accurately model the clear-sky values of the infrared absorption channels. The ability to perform the physical retrievals outlined in this document requires an accurate forward model, accurate ancillary data and well-characterized spectral response functions.

ALGORITHM DESCRIPTION

1.8 Algorithm Overview

The ACHA serves a critical role in the GOES-R ABI processing system. It provides a fundamental cloud property but also provides information needed by other cloud and non-cloud algorithms. As such, latency was a large concern in developing the ACHA. The current version of the ACHA algorithm draws on the following heritage algorithms:

- The CLAVR-x split-window cloud height from NESDIS, and
- The MODIS CO_2 cloud height algorithm developed by the UW/CIMSS.

The ACHA derives the following ABI cloud products listed in the F&PS:

- Cloud-top temperature,
- Cloud-top pressure,
- Cloud-top height, and
- Cloud cover layer.

All of these products are derived at the pixel level for all cloudy pixels.

In addition, the ACHA derives the following products that are not included in F&PS:

- Quality flags,
- Cloud 11 μm emissivity, and
- Cloud microphysical index (β).

Section 3.4 describes the full set of outputs from the ACHA algorithm.

1.9 Processing Outline

The processing outline of the ACHA is summarized in Figure 1. The current ACHA is implemented with the NOAA/NESDIS/STAR GOES-R AIT processing framework (FRAMEWORK). FRAMEWORK routines are used to provide all of the observations and ancillary data. The ACHA is designed to run on segments of data where a segment is comprised of multiple scan lines.

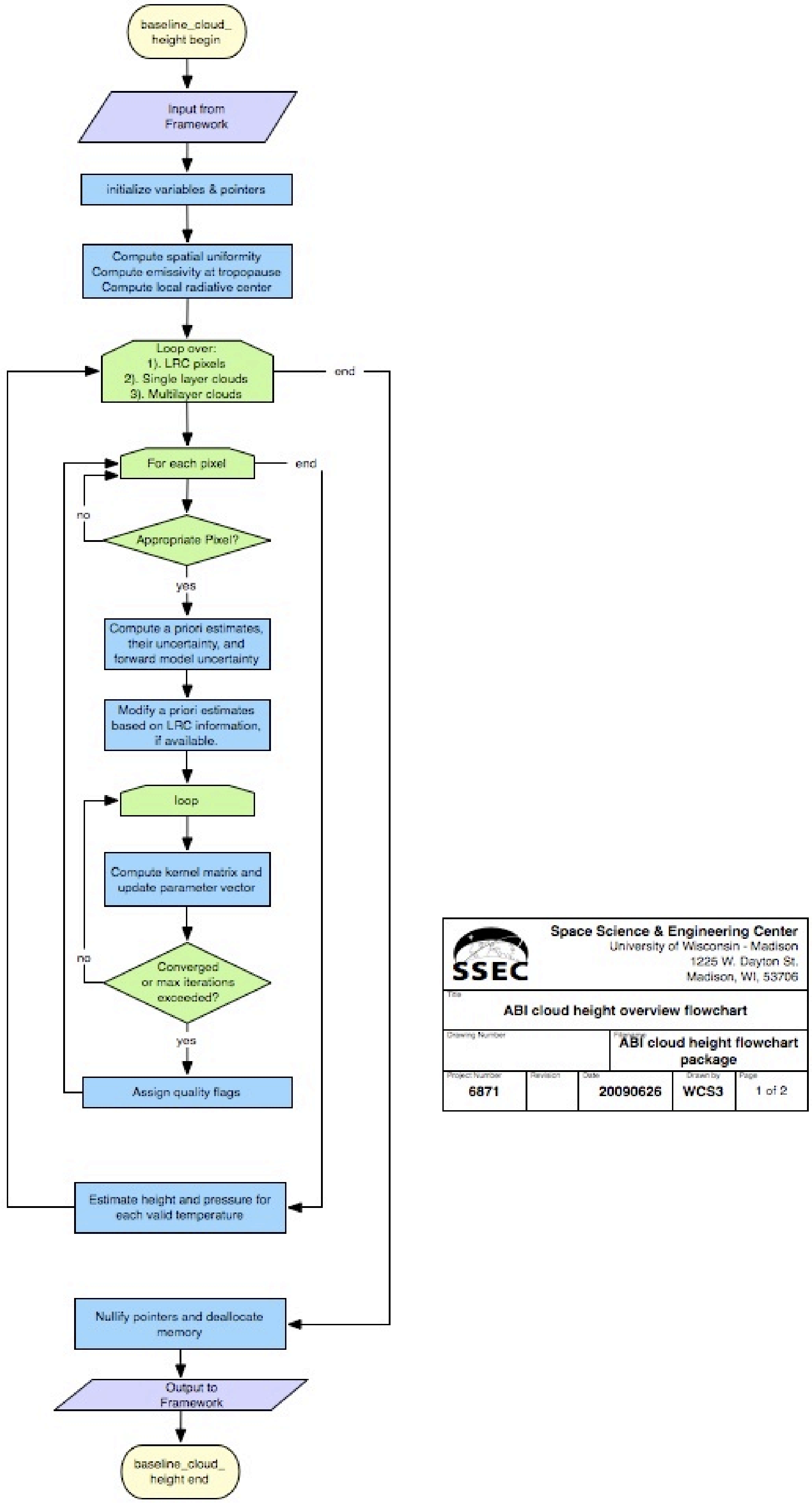
baseline_cloud_ height begin
Input from Framework
initialize variables & pointers
Compute spatial uniformity
Compute emissivity at tropopause
Compute local radiative center
Loop over:
1). LRC pixels
2). Single layer clouds
3). Multilayer clouds
end
For each pixel
end
no
Appropriate Pixel?
yes
Compute a priori estimates, their uncertainty, and forward model uncertainty
Modify a priori estimates based on LRC information, if available.
loop
Compute kernel matrix and update parameter vector
no
Converged or max iterations exceeded?
yes
Assign quality flags
Estimate height and pressure for each valid temperature
Nullify pointers and deallocate memory
Output to Framework
baseline_cloud_ height end
SSEC
Space Science & Engineering Center
University of Wisconsin - Madison
1225 W. Dayton St.
Madison, WI, 53706
Title
ABI cloud height overview flowchart
Drawing Number
Filename
ABI cloud height flowchart package
Project Number
6871
Revision
Date
20090626
Drawn by
WCS3
Page
1 of 2

Figure 1 High level flowchart of the ACHA illustrating the main processing sections.

1.10 Algorithm Input

This section describes the input needed to process the ACHA. In its current configuration, the ACHA runs on segments comprised of 200 scan lines. While this is the ideal number of scan-lines per segment the ACHA algorithm should be run on, the algorithm does benefit from running on larger number of scan-lines. The ACHA must be run on arrays of pixels because spatial uniformity of the observations is necessary to the algorithm. In addition, the final algorithm design will include separate loops over those pixels in the segment determined to be local radiative centers (LRC), those pixels determined by the cloud typing algorithm to be single-layer clouds and those pixels determined to multi-layer clouds. The calculation of the LRC, which is done by the gradient filter, is described in the AIADD. The following sections describe the actual input needed to run the ACHA.

1.10.1 Primary Sensor Data

The list below contains the primary sensor data used by the ACHA. By primary sensor data, we mean information that is derived solely from the ABI observations and geolocation information.

- Calibrated radiances for channels 14.
- Calibrated brightness temperatures for channels 14, 15 and 16.
- Cosine of local zenith angle
- Local zenith angle
- Space mask
- Bad pixel mask for channels 14, 15, and 16

1.10.2 Ancillary Data

The following lists the ancillary data required to run the ACHA. A more detailed description is provided in the AIADD. By ancillary data, we mean data that require information not included in the ABI observations or geolocation data.

- **Surface elevation**
- **Surface Type**
- **NWP level associated with the surface**
- **NWP level associated with the tropopause**
- **NWP tropopause temperature**
- **Profiles of height, pressure and temperature from the NWP**

- **Inversion level profile from NWP**
- **Surface temperature and pressure from NWP**
- **Local Zenith Angle bin**
- **NWP Line and element indices**
- **Clear-sky transmission, and radiance profiles for channels 14, 15 and 16 from the RTM**
- **Blackbody radiance profiles for channels 14, 15 and 16 from the RTM**
- **Clear-sky estimates of channel 14, 15 and 16 radiances from the RTM**

1.10.3 Derived Data

The following lists and briefly describes the data that are required by the ACHA that is provided by other algorithms.

- **Cloud Mask**
  A cloud mask is required to determine which pixels are cloudy and which are not, which in turn determines which pixels are processed. This information is provided by the ABI Cloud Mask (ACM) algorithm. Details on the ACM are provided in the ACM ATBD.

- **Cloud Type/Phase**
  A cloud type and phase are required to determine which *a priori* information for the forward model are used. It is assumed that both the cloud type and phase are inputs to the ACHA algorithm. These products are provided by the ABI Cloud Type/Phase Algorithm. Information on the ABI Cloud Type/Phase is provided in the ABI Type/Phase ATBD.

- **Local Radiative Centers**
  Given a derived channel 14 top of troposphere emissivity, $\varepsilon_{stropo}(11\mu m)$, the local radiative center (LRC) is defined as the pixel location, in the direction of the gradient vector, upon which the gradient reverses or when an emissivity value ($\varepsilon_{stropo}(11\mu m)$) greater than or equal to 0.75 is found, whichever occurs first. The gradient filter routine is required as an input to the ACHA. The method to compute the gradient function is described in Pavolonis (2009) and in the AIADD. The required inputs to the gradient filter are:
    - $\varepsilon_{stropo}(11\mu m)$,
    - The line and element size of the segment being processed,
    - A binary mask for the segment of pixels that have non-missing $\varepsilon_{stropo}(11\mu m)$ for the segment,

  - The minimum and maximum valid emissivity values (0.0 and 1.0 respectively), and
  - The maximum ε_{stropo}(11μm) value to be considered (0.75).

  The outputs from the gradient filter are the line and element of the LRC. A further description of how the LRC is calculated can be found in the AIADD. After the LRC Line/Element are computed using the LRC algorithm for each pixel of a given segment (as described in the AIADD), a further check is performed. If the derived 11 μm top of troposphere emissivity is greater than the gradient threshold (0.75) for a given pixel, then the LRC line/element is set to the current pixel line/element.

- **Derived channel 14 top of troposphere emissivity**
  The ACHA requires knowledge of the channel 14 emissivity of a cloud assuming that its top coincides with the tropopause. This calculation is done by using the measured channel 14 radiance, clear sky channel 14 radiance from the RTM, space mask, latitude/longitude cell index from the NWP, tropopause index from the NWP, local zenith angle bin index, and channel 14 μm blackbody radiance.

- **Spatial uniformity information**
  The following pieces of information are calculated using the spatial uniformity algorithm, as described in the AIADD. Since piece is computed over a segment of data, the input array is assumed to be a segment of data. All of the calls require the space mask for the current segment of data as well as dx = dy = 1 (NOTE: dx = dy = 1 means that the spatial uniformity will be performed over a 3x3 set of pixels, centered on the current pixel. See the AIADD description for more detail). While the spatial uniformity algorithm outputs the mean, maximum, minimum and standard deviation, the following are used in the ACHA. Because the spatial uniformity outputs are calculated for a segment of data, the function is called prior to processing the ACHA algorithm. The pixel level outputs are used as described in the appropriate sections of this ATBD.

  - Standard deviation channel 14 brightness temperature over a 3x3 array ($\sigma_{BT(11\mu m)}$)
    - Input: Current segment of channel 14 brightness temperatures.
  - Standard deviation of channel 14-15 brightness temperature difference over a 3x3 array ($\sigma_{BTD(11\text{-}12\mu m)}$)
    - Input: Current segment of channel 14 -15 brightness temperature differences
  - Standard deviation channel 14-16 brightness temperature difference over a 3x3 array ($\sigma_{BTD(11\text{-}13\mu m)}$)
    - Input: Current segment of channel 14 -15 brightness temperature differences.
- .

1.11 Theoretical Description

As described below, the ACHA represents an innovative approach that uses multiple IR channels within algorithm that provides results that are consistent for all viewing conditions. This approach combines multiple window channel observations with a single absorption channel observations to allow for estimation of cloud height without large assumptions on cloud microphysics for the first time from a geostationary imager. The remainder of this section provides the physical basis for the chosen approach.

1.11.1 Physics of the Problem

The ACHA uses the infrared observations from the ABI to extract the desired information on cloud height. Infrared observations are impacted not only by the height of the cloud, but also its emissivity and how the emissivity varies with wavelength (a behavior that is tied to cloud microphysics). In addition, the emissions from the surface and the atmosphere can also be major contributors to the observed signal. Lastly, clouds often exhibit complex vertical structures that violate the assumptions of the single layer plane parallel models (leading to erroneous retrievals). The job of the ACHA is to exploit as much of the information provided by the ABI as possible with appropriate, computationally efficient and accurate methods to derive the various cloud height products.

1.11.1.1 Motivation for ACHA Channel Selection

The ACHA represents a merger of current operational cloud height algorithms run by NESDIS on the Polar Orbiting Environmental Satellite (POES) and GOES imagers. The current GOES-NOP cloud height algorithm applies the CO_2 slicing method to the 11 and 13.3 μm observations. This method is referred to as the CO_2/IRW approach. CO_2 slicing was developed to estimate cloud-top pressures using multiple channels typically within the 14 μm CO_2 absorption band. For example, the MODIS MOD06 algorithm (Menzel et al., 2006) employs four CO_2 bands, and the GOES Sounder approach also employs four bands. CO_2 slicing benefits from the microphysical simplicity provided by the spectral uniformity of the cloud emissivity across the 14 μm band. The GOES-NOP method suffers from two weaknesses relative to the MOD06 method. First, the assumption of spectral uniformity of cloud emissivity is not valid when applied to the 11 and 13.3 μm observations. Second, the 13.3 μm channel does not provide sufficient atmospheric opacity to provide the desired sensitivity to cloud height for optically thin high cloud (i.e., cirrus). For optically thick clouds, CO_2 slicing methods rely simply on the 11 μm observation for estimating the cloud height.

In contrast to the CO_2/IRW approach used for GOES-NOP, the method employed operationally for the POES imager (AVHRR) uses a split-window approach based on the 11 and 12 μm observations. Unlike the 13.3 μm band, the 11 and 12 μm bands are in spectral windows and offer little sensitivity to cloud height for optically thin cirrus. As described in Heidinger and Pavolonis (2009), the split-window approach does provide accurate measurements of cloud emissivity and its spectral variation.

Unlike the GOES-NOP imager or the POES Imager, the ABI provides the 13.3 µm CO_2 channels coupled with multiple longwave IR windows (10.4, 11 and 12 µm). The ABI therefore provides an opportunity to combine the sensitivity to cloud height offered by a CO_2 channel with the sensitivity to cloud microphysics offered by window channels and to improve upon the performance of the cloud height products derived from the current operational imagers.

To demonstrate the benefits of the ACHA CO_2/Split-Window algorithm, the sensitivity to cloud pressure offered by the channels used in the ACHA was compared to other channel sets using co-located MODIS and CALIPSO observations. These results where taken from Heidinger et al. (2010). Figure 2 shows a false color image from AQUA/MODIS for a cirrus scene observed on August 10, 2006 over the Indian Ocean. The red line in Figure 2 shows the location of the CALIPSO track. This scene is characterized by a predominantly single cirrus cloud of varying optical thickness with thicker regions on the left-side of the figure. An image of the 532 nm CALIPSO data for the trajectory shown in Figure 2 is shown in Figure 3.

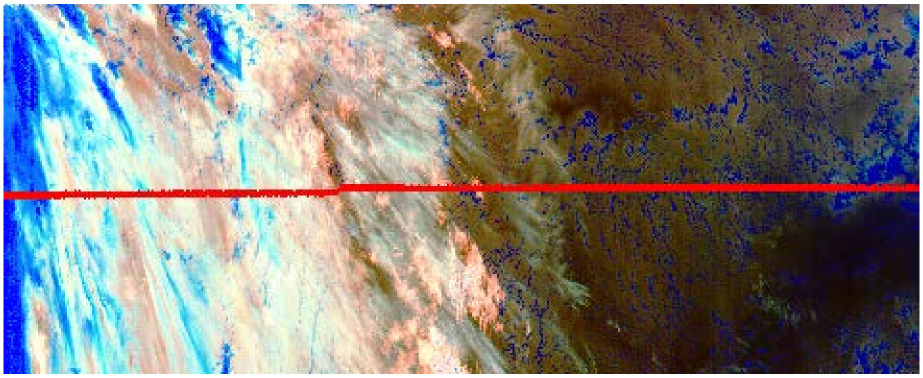

Figure 2 A false color image constructed from 11 – 12µm BTD (Red), 4 – 11µm BTD (Green) and 11 µm BT reversed (Blue). Data are taken from AQUA/MODIS and CALIPSO/CALIOP on August 10, 2006 from 20:35 to 20:40 UTC. The red line is the CALIPSO track. In this color combination, cirrus clouds appear white but as the optical thickness increases, the ice clouds appear as light blue/cyan. Low-level water clouds appear as dark blue, and mid-level water clouds tend to have a red/orange color.

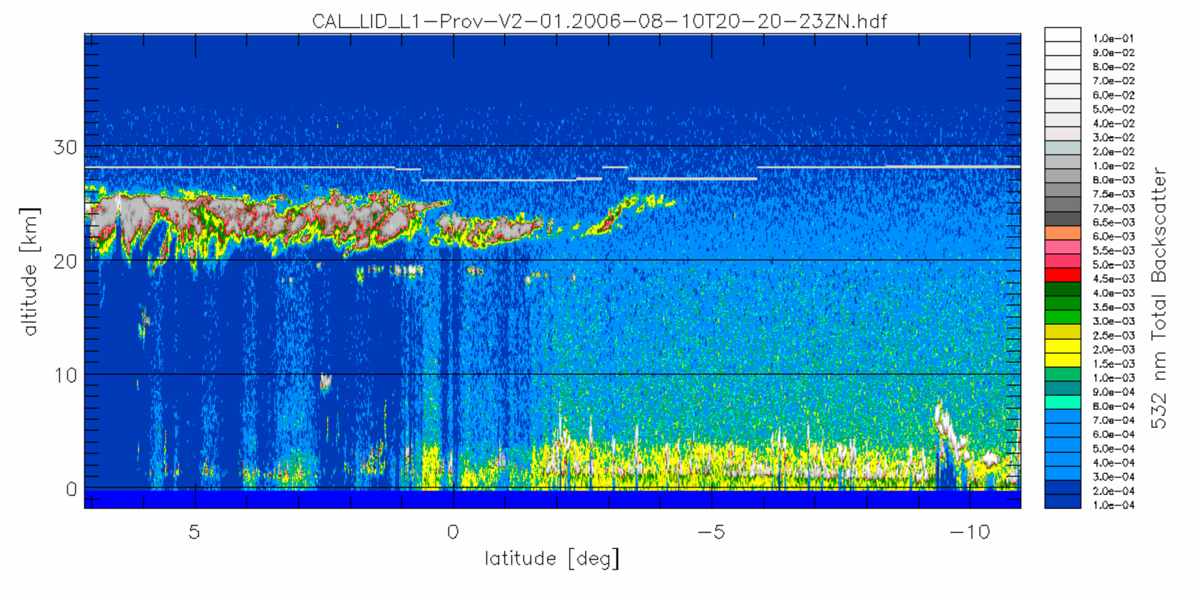

Figure 3 The 532 nm total backscatter from CALIOP along the red line shown in Figure 2. The grey line in the centre image is the Tropopause.

In the work of Heidinger et al. (2009), an analysis was applied to the above data to study the impact on the cloud-top pressure solution space offered by various channel combinations commonly used on operational imagers. The term solution space refers to the vertical region in the atmospheric column where a cloud can exist and match the observations of the channels used in the algorithm. As described in Heidinger et al. (2009) this analysis was accomplished specifically by computing the emissivity profiles for each channel and determining the levels at which the emissivities were all valid and where the spectral variation of the emissivities was consistent with the chosen scattering model. It is important to note that this analysis was not a comparison of algorithms, but a study of the impact of the pixel spectral information on the possible range of solutions.

Figure 4 shows the resulting computation of the cloud-top pressure solution space spanned by the ACHA CO_2/Split-Window algorithm (channels 14, 15 & 16). The grey area represents the region of the atmosphere where the MODIS observations of those channels were matched to within 0.5K. The blue points represent the cloud-top pressures where the cloud matched the MODIS observation most closely. In contrast, Figure 5 shows the same computation when using the VIIRS cloud-top height algorithm’s channel set. As described by Heidinger et al. (2009), the large improvement in the sensitivity to cloud top pressure seen in ACHA versus the VIIRS algorithm is due to the presence of the CO_2 absorption channel. Because VIIRS offers only IR window channels, its ability to estimate the height of cirrus clouds with confidence is limited.

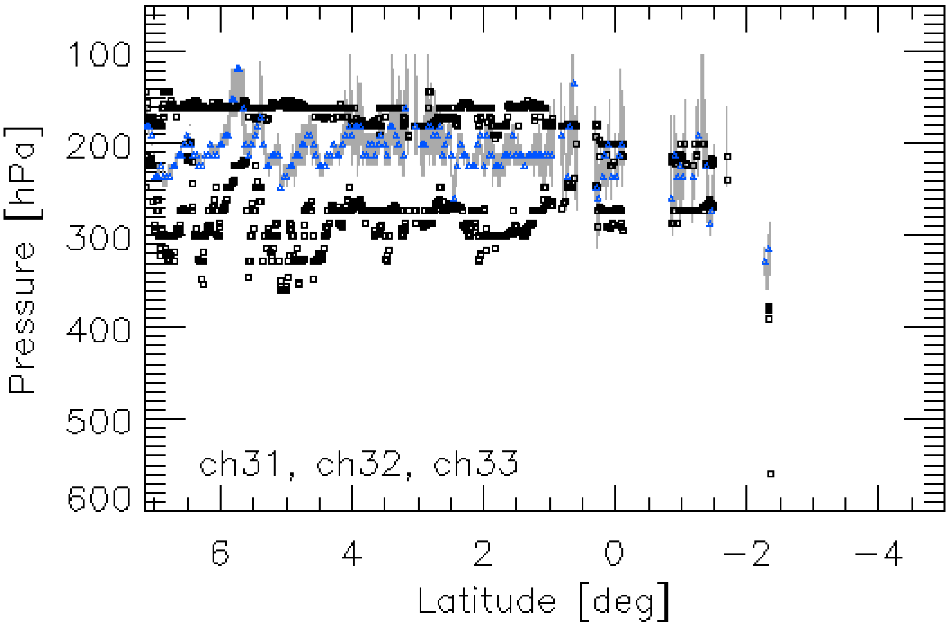

Figure 4 Cloud-top pressure solution space provided by the ACHA channel set for the ice clouds along the CALIPSO track for August 10, 2006 20:35 – 20:40 UTC. The grey lines represent the solution space provided by the selected GOES-R ABI channels. The black symbols provide the CALIOP cloud boundaries for the highest cloud layer. The blue points represent the location of the optimal cloud-top pressure solutions with this channel set. For clarity, only every fifth optimal cloud-top pressure solution is plotted.

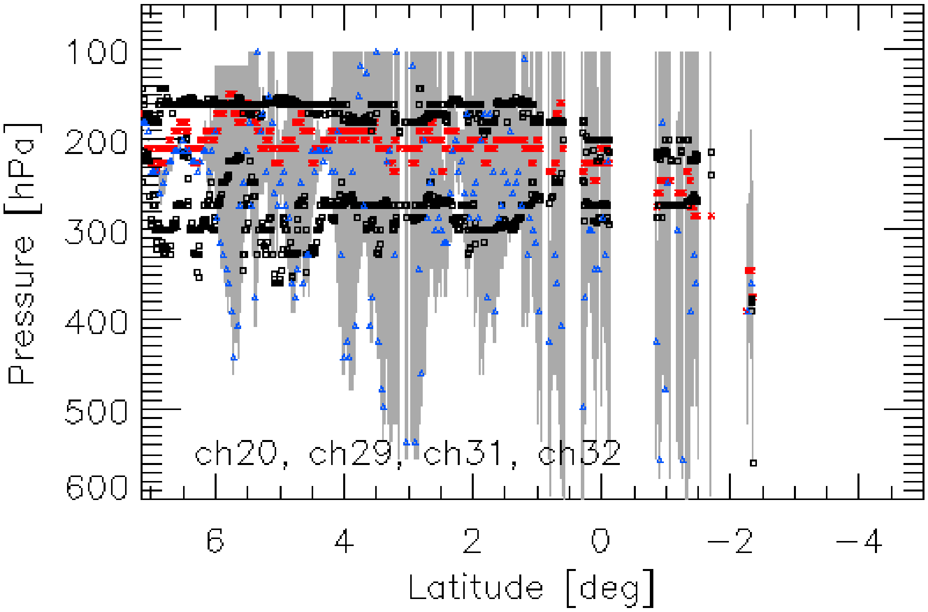

Figure 5 Same as Figure 4 computed for the VIIRS channel set (3.75, 8.5, 11 and 12 µm). Red points show the MODIS (MYD06) results for reference.

1.11.1.2 Radiative Transfer Equation

The radiative transfer equation (1) employed here is given as

$$R_{obs} = e_c R_{ac} + t_{ac} e_c \, \mathrm{B}(T_c) + R_{clr}(1 - e_c) \quad \text{(Eq. 1)}$$

where R_{obs} is the observed top-of-atmosphere radiance, T_c is the cloud temperature, B() represents the Planck Function and R_{clr} is the clear-sky radiance (both measured at the top of the atmosphere). R_{ac} is the above-cloud emission; t_{ac} is the above-cloud transmission along the path from the satellite sensor to the cloud pixel. Finally, the cloud emissivity is represented by e_c. All quantities in Eq. 1 are a function of wavelength, λ, and are computed separately for each channel.

As described later, the 11 μm cloud emissivity is directly retrieved by the ACHA. The 12 and 13.3 μm cloud emissivities are not retrieved but they are utilized during the retrieval process.

To account for the variation of e_c with each channel, the β parameter is evoked. For any two-channel pair (1,2), the value of β can be constructed using the following relationship:

$$\beta_{1,2} = \ln(1 - e_2) \big/ \ln(1 - e_1) \quad \text{(Eq. 2)}$$

Using this relationship, the cloud emissivities at 12 and 13 um can be derived from the cloud emissivity value at 11 μm as follows:

$$e_c(12\mu m) = 1 - [1 - e_c(11\mu m)]^{\beta(12/11\mu m)} \quad \text{(Eq. 3)}$$

$$e_c(13.3\mu m) = 1 - [1 - e_c(11\mu m)]^{\beta(13.3/11\mu m)} \quad \text{(Eq. 4)}$$

For the remainder of this document, the value of e_c will refer to the cloud emissivity at 11 μm and β will refer to the β(11/12μm) value unless stated otherwise. β is a convenient parameter because it also provides a direct link to cloud microphysics which is discussed in the next section.

While the above radiative transfer equation is simple in that it assumes no scattering and that the cloud can be treated as a single layer, it does allow for semi-analytic derivations of the observations to the controlling parameters (i.e., cloud temperature). This behavior is critical because it allows for an efficient retrieval without the need for large lookup tables.

1.11.1.3 Cloud Microphysical Assumptions

One of the strengths of the ACHA is that it allows cloud microphysics to vary during the retrieval process which should improve the cloud height estimates (Heidinger et al., 2009). Cloud microphysics is included in the retrieval through the spectral variation of the β parameters. The variation of β between different channel pairs is a function of particle size and ice crystal habit. For example, Parol et al. (1991) showed that β can be related to the scattering properties using the following relationship where ω is the single scattering albedo, g is the asymmetry parameter and σ_{ext} is the extinction coefficient:

$$\beta_{2,1} = \frac{[1.0 - \omega(\lambda_1) g(\lambda_1)]\sigma_{ext}(\lambda_1)}{[1.0 - \omega(\lambda_2) g(\lambda_2)]\sigma_{ext}(\lambda_2)} \quad \text{(Eq. 5)}$$

This relationship between β and the scattering properties will allow the ACHA to estimate cloud particle size from the retrieved β values.

While the scattering properties for water clouds are well modeled by Mie theory, the scattering properties of ice clouds are less certain. To define a relationship between the β values for ice clouds, assumptions have to be made about the ice crystals. In the ACHA, we use the ice scattering models provided by Professor Ping Yang at Texas A&M University (Yang et al., 2005). In this database, ice models are separated by habits. To pick a habit, β values were computed using MODIS observations collocated with CALIPSO. We then compared how the observed β values corresponded with those computed from the scattering. The results indicated that aggregates modeled the observed data the best. The image below (Figure 6) shows this analysis which was generated for August 2006. For water clouds, standard Mie theory computed scattering properties are used to predict the β values and their relationship with each other.

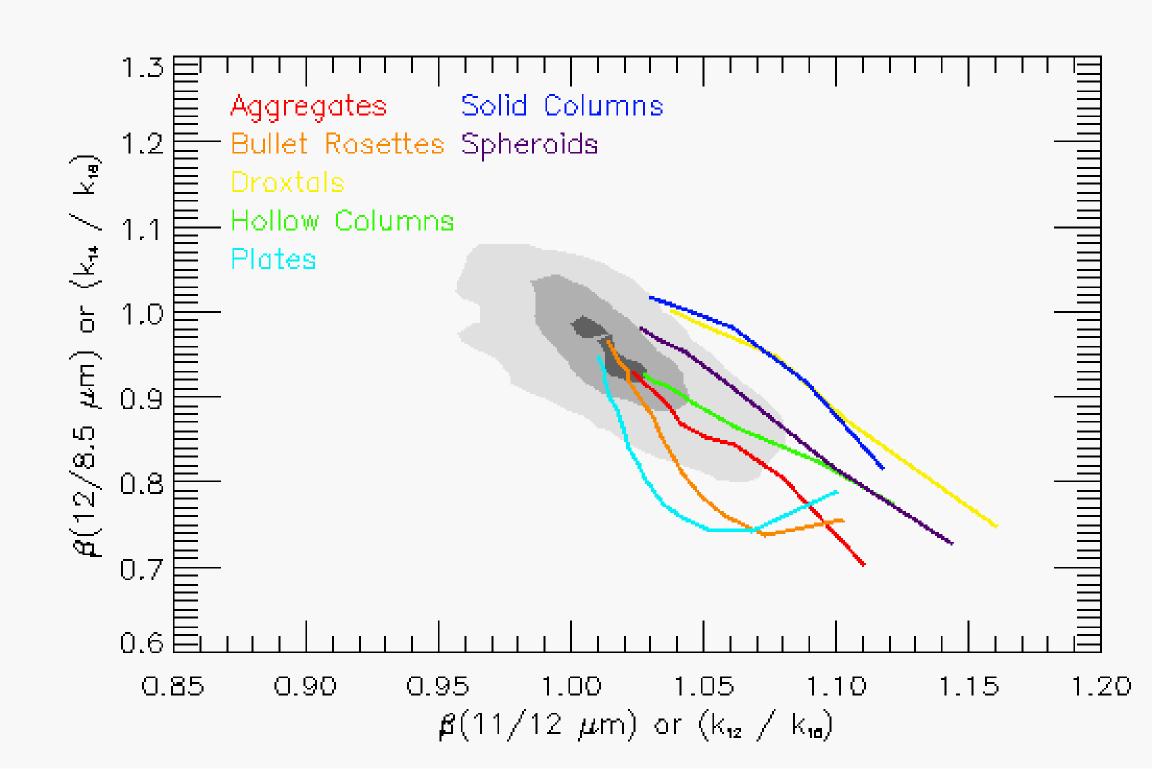

Figure 6 Comparison of the variation of β values for 11 and 12 µm against those for 12 and 8.5 µm. The cloud of points represents those computed using CALIPSO observations collocated with MODIS. The lines represent predictions based on the Yang et. al scattering database.

Once the habit has been determined, the needed β relationships can be computed. Figure 7 shows the computed variation of the 11 and 12 µm β with the 11 and 11.3 µm β and Figure 8 shows the variation of the 11 and 12 µm β with particle size. These curves and the regressions shown in Figure 7 and Figure 8 are used directly in the optimal estimation approach described in the next session.

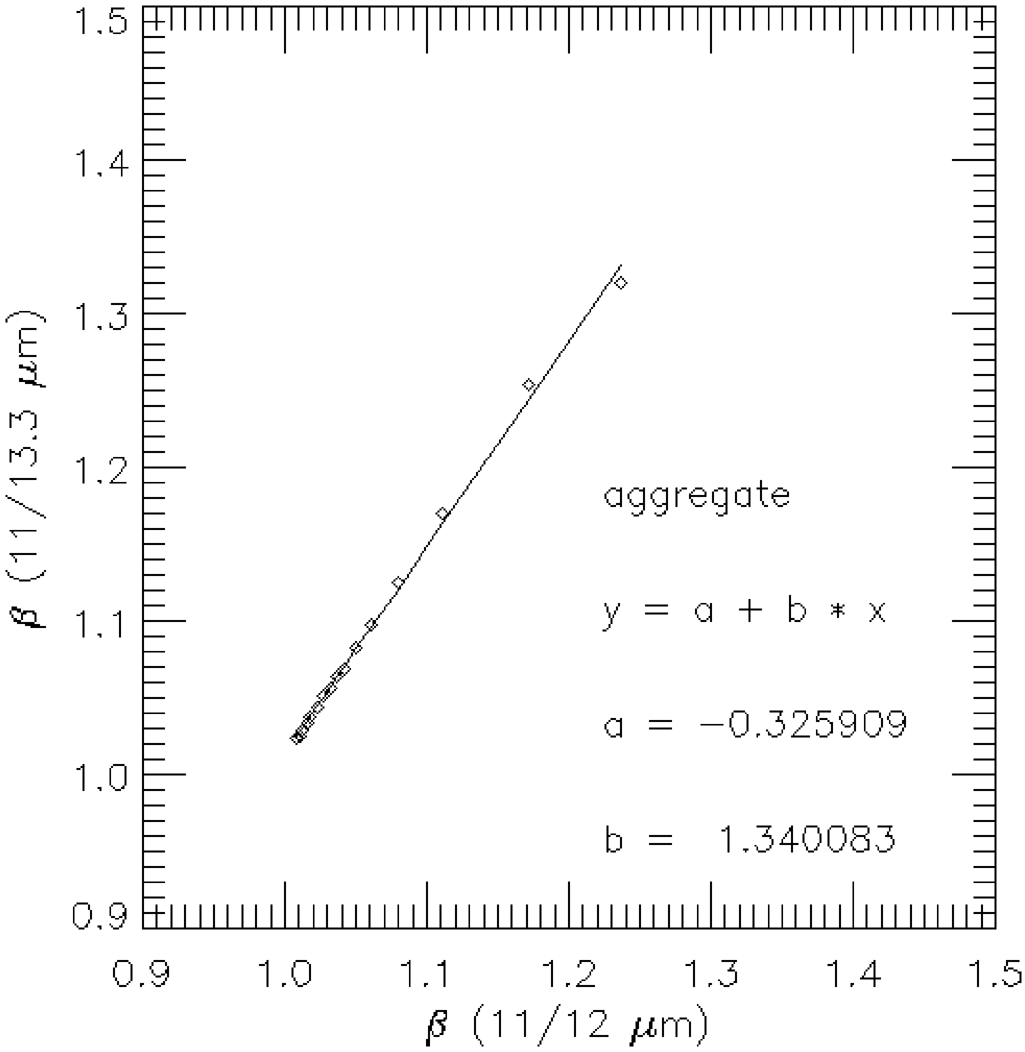

Figure 7 Computed variation and linear-fit of the 11 and 13.3 μm β values to those computed using 11 and 12 μm. β is a fundamental measure of the spectral variation of cloud emissivity, and this curve is used in the forward model in the retrieval. The data shown are for ice crystals with an aggregate habit. For water clouds, Mie theory predicts a = -0.217 and b = 1.250.

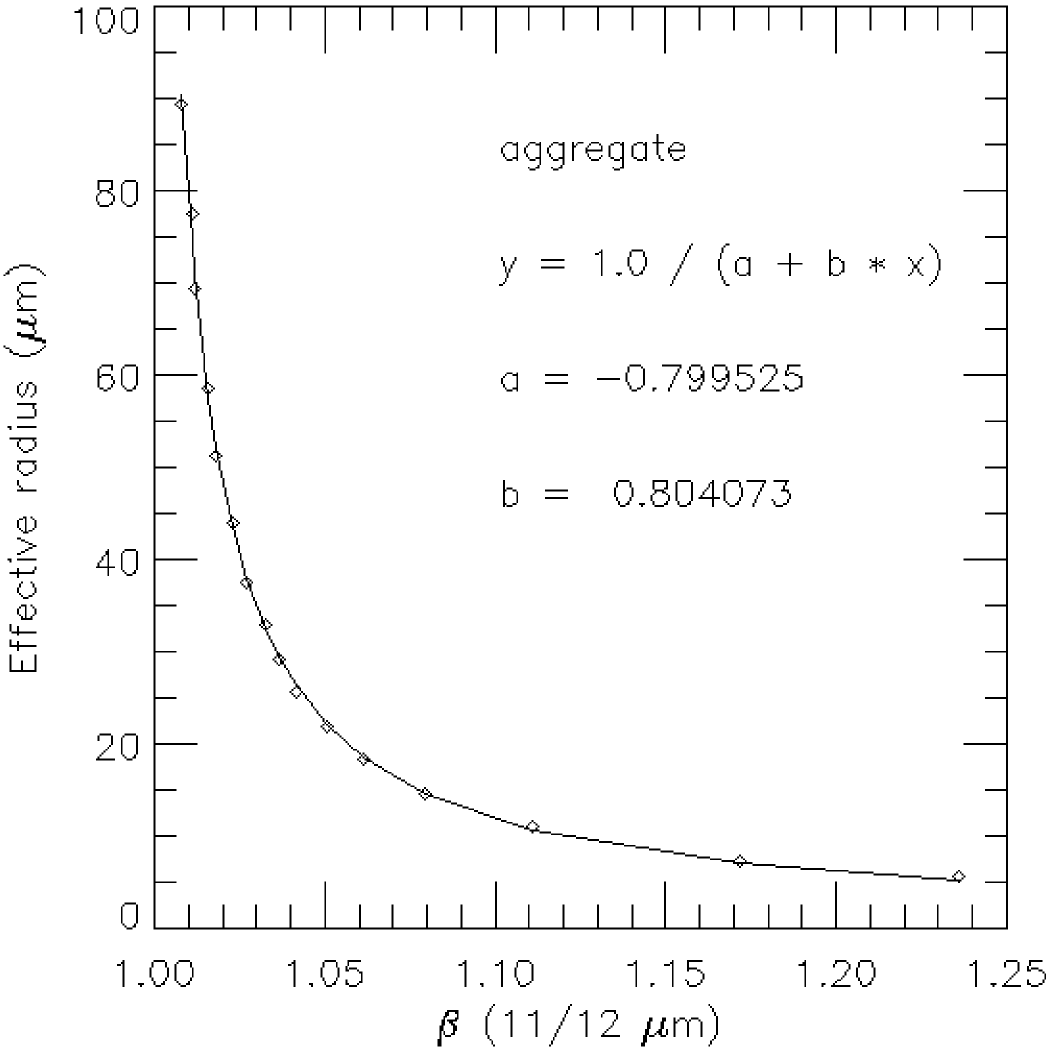

Figure 8 Variation of the 11 and 12 μm β values as a function of the ice crystal radius. This relation is used in the retrieval to produce an estimate of cloud particle size from the final retrieved β values.

1.11.2 Mathematical Description

The mathematical approach employed here is the optimal estimation approach described by Rodgers (1976). The optimal estimation approach is also often referred to as a 1DVAR approach. The benefits of this approach are that it is flexible and allows for the easy addition or subtraction of new observations or retrieved parameters. Another benefit of this approach is that it generates automatic estimates of the retrieval errors. The following description of the method employs the same notation as Rodgers (1976) but provides only a brief review.

The optimal estimation (3) approach minimizes a cost function, **Φ**, given by

$$\phi = (x - x_a)^T S_a^{-1}(x - x_a) + (y - f(x))^T S_y^{-1}(y - f(x)) \quad \text{(Eq. 6)}$$

where **x** is a vector of retrieved parameters, $\mathbf{x_a}$ is a vector housing the *a priori* values of **x** (which also serve as a first guess to begin iterations to a convergent solution), **y** is the vector of observations, and **f** is the forward model's estimates of the values of **y** under the assumptions of state **x**. $\mathbf{S_a}$ is the error covariance matrix corresponding to the values of $\mathbf{x_a}$, and $\mathbf{S_y}$ is the error covariance matrix for the forward model and measurements.

In each retrieval iteration, up to a maximum number of 10 iterations, the state vector **x** is incremented as follows:

$$\delta x = S_x\left(K^T\left(S_y^{-1}[y - f(x)] + S_a^{-1}(x_a - x)\right)\right) \quad \text{(Eq. 7)}$$

where **K** is the Jacobian or Kernel matrix (whose computation is described below) and $\mathbf{S_x}$ is the covariance error matrix of **x** which is computed as

$$S_x = (S_a^{-1} + K^T S_y^{-1} K)^{-1}. \quad \text{(Eq. 8)}$$

The retrieval iterations are conducted until the following criterion is met:

$$\left\| \sum \delta x S_x^{-1} \delta x \right\| \le \frac{p}{2} \quad \text{(Eq. 9)}$$

where ***p*** is the number of elements in ***x***. After the convergence criteria is met, the retrieval vector is updated.

In ACHA, the **y** and **x** vectors are defined as follows.

$$y = \begin{pmatrix} BT(11\mu m) \\ BTD(11-12\mu m) \\ BTD(11-13.3\mu m) \end{pmatrix} \quad \text{(Eq. 10)}$$

$$x = \begin{pmatrix} T_c \\ e(11\mu m) \\ \beta(12/11\mu m) \end{pmatrix} \quad \text{(Eq. 11)}$$

$$x_a = \begin{pmatrix} T_c\_ap \\ e(11\mu m)\_ap \\ \beta(12/11\mu m)\_ap \end{pmatrix} \quad \text{(Eq. 12)}$$

The Kernel matrix contains the partial derivatives of each element of **f(x)** to each element of **x**. In Heidinger and Pavolonis (2009), the equations defining all of the elements of **K** except those that involve the 13.3 mm channel are given. The following relationships repeat those in Heidinger and Pavolonis (2009) and provide the remaining terms used in the ACHA.

$$K = \begin{pmatrix} \frac{\partial BT(11\mu m)}{\partial T_{eff}} & \frac{\partial BT(11\mu m)}{\partial e(11\mu m)} & \frac{\partial BT(11\mu m)}{\partial \beta(12/11\mu m)} \\ \frac{\partial BTD(11-12\mu m)}{\partial T_{eff}} & \frac{\partial BTD(11-12\mu m)}{\partial e(11\mu m)} & \frac{\partial BTD(11-12\mu m)}{\partial \beta(12/11\mu m)} \\ \frac{\partial BTD(11-13.3\mu m)}{\partial T_{eff}} & \frac{\partial BTD(11-13.3\mu m)}{\partial e(11\mu m)} & \frac{\partial BTD(11-13.3\mu m)}{\partial \beta(12/11\mu m)} \end{pmatrix} \quad \text{(Eq. 13)}$$

The expressions required for the first column of ***K*** are given by Eqs. 14-16.

$$\frac{\partial BT(11\mu m)}{\partial T_c} = e_c(11\mu m)t_{ac}(11\mu m)\left(\frac{\partial B(11\mu m)}{\partial T_c}\right)\left(\frac{\partial B(11\mu m)}{\partial T}\right)^{-1} \quad \text{(Eq. 14)}$$

$$\frac{\partial BTD(11-12\mu m)}{\partial T_c} = \frac{\partial BT(11\mu m)}{\partial T_c} - e_c(12\mu m)t_{ac}(12\mu m)\left(\frac{\partial B(12\mu m)}{\partial T_c}\right)\left(\frac{\partial B(12\mu m)}{\partial T}\right)^{-1} \quad \text{(Eq. 15)}$$

$$\begin{aligned} &\frac{\partial BTD(11-13.3\mu m)}{\partial T_{eff}} = \\ &\frac{\partial BT(11\mu m)}{\partial T_c} - e_c(13.3\mu m)t_{ac}(13.3\mu m)\left(\frac{\partial B(13.3\mu m)}{\partial T_c}\right)\left(\frac{\partial B(13.3\mu m)}{\partial T}\right)^{-1} \end{aligned} \quad \text{(Eq. 16)}$$

The expressions for the second column of ***K*** are given by Eqs. 17-19.

$$\frac{\partial BT(11\mu m)}{\partial e_c(11\mu m)} = [R_{cld}(11\mu m) - R_{clr}(11\mu m)]\left(\frac{\partial B(11\mu m)}{\partial T}\right)^{-1} \quad \text{(Eq. 17)}$$

$$\begin{aligned} &\frac{\partial BTD(11-12\mu m)}{\partial e_c(11\mu m)} = \\ &\frac{\partial BT(11\mu m)}{\partial e_c(11\mu m)} - [R_{cld}(12\mu m) - R_{clr}(12\mu m)][\beta(12/11\mu m)(1-e_c(11\mu m))^{\beta(12/11\mu m)-1}]\left(\frac{\partial B(12\mu m)}{\partial T}\right)^{-1} \end{aligned}$$

(Eq. 18)

$$\frac{\partial BTD(11-13.3\mu m)}{\partial e_c(11\mu m)} =$$

$$\frac{\partial BT(11\mu m)}{\partial e_c(11\mu m)} - [R_{cld}(13.3\mu m) - R_{clr}(13.3\mu m)][\beta(13.3/11\mu m)(1-e_c(11\mu m))^{\beta(13.3/11\mu m)-1}]\left(\frac{\partial B(13.3\mu m)}{\partial T}\right)^{-1}$$

(Eq. 19)

Finally, the derivative of each forward model simulation with respect to β(12/11μm) is given by the following equations:

$$\frac{\partial BT(11\mu m)}{\partial \beta(12/11\mu m)} = 0.0$$ (Eq. 20)

$$\frac{\partial BTD(11-12\mu m)}{\partial \beta(12/11\mu m)} = [R_{cld}(12\mu m) - R_{clr}(12\mu m)]\ln[1-e_c(11\mu m)][1-e_c(12\mu m)]\left(\frac{\partial B(12\mu m)}{\partial T}\right)^{-1}$$

(Eq. 21)

$$\frac{\partial BTD(11-13.3\mu m)}{\partial \beta(12/11\mu m)} =$$

$$[R_{cld}(13.3\mu m) - R_{clr}(13.3\mu m)]\ln[1-e_c(11\mu m)][1-e_c(13.3\mu m)]\left(\frac{\partial \beta(13.3/11\mu m)}{\partial \beta(12/11\mu m)}\right)\left(\frac{\partial B(13.3\mu m)}{\partial T}\right)^{-1}$$

(Eq. 22)

The values of $\partial \beta_{11/13} / \partial \beta_{11/12}$ are computed using the regression shown in Figure 6. For water clouds, the same form of a regression shown in Figure 6 is used except that the a-coefficient is -0.217 and the b-coefficient is 1.250.

1.11.2.1 Estimation of Prior Values and their Uncertainty

The proper implementation of ACHA requires meaningful estimates of *a priori* values housed in $\boldsymbol{x_a}$ and their uncertainties housed in $\boldsymbol{S_a}$. $\boldsymbol{S_a}$ is a two-dimensional matrix with each dimension being the size of $\boldsymbol{x_a}$. For the ACHA, we assume $\boldsymbol{S_a}$ is a diagonal matrix with each element being the assumed variance of each element of $\boldsymbol{x_a}$ as illustrated below.

$$S_a = \begin{pmatrix} \sigma^2_{Tc\_ap} & 0.0 & 0.0 \\ 0.0 & \sigma^2_{\varepsilon(11\mu m)\_ap} & 0.0 \\ 0.0 & 0.0 & \sigma^2_{\beta(12/11\mu m)\_ap} \end{pmatrix}$$ (Eq. 23)

In the ACHA, we currently use the *a priori* estimate of $\boldsymbol{x_a}$ and $\boldsymbol{S_a}$ given by Heidinger and Pavolonis (2009). In this paper, CALIPSO-derived values of T_c, e_c, and β are derived, and distributions are computed for the various cloud types generated by the GOES-R AWG cloud typing algorithm. The means and standard deviations of these distributions are used for the values of $\boldsymbol{x_a}$ and $\boldsymbol{S_a}$ for the non-opaque cloud types (cirrus and multi-layer). For the opaque cloud types, the *a priori* values of T_c are provided by the 11 μm brightness temperature. The *a priori* values of β are taken from scattering theory and are set to 1.1 for ice-phase clouds and 1.3 for water-phase clouds. The standard deviation of β is assumed to be 0.2 based on the distributions of Heidinger and Pavolonis (2009).

1.11.2.2 Estimation of Forward Model Uncertainty

This section describes the estimation of the elements of $\boldsymbol{S_y}$ which contain the uncertainty expressed as a variance of the forward model estimates. As was the case with $\boldsymbol{S_a}$, $\boldsymbol{S_y}$ is assumed be a diagonal matrix. As our experience with the ACHA grows, the computation of the off-diagonal will be explored.

Assumed to be diagonal, $\boldsymbol{S_y}$ can be expressed as follows:

$$S_y = \begin{pmatrix} \sigma^2_{BT(11\mu m)} & 0.0 & 0.0 \\ 0.0 & \sigma^2_{BTD(11-12\mu m)} & 0.0 \\ 0.0 & 0.0 & \sigma^2_{BTD(11-13.3\mu m)} \end{pmatrix} \quad \text{(Eq. 24)}$$

The variance terms are computed by summing up three components:

$$\sigma^2 = \sigma^2_{instr} + [1 - e_c(11\mu m)]\sigma^2_{clr} + \sigma^2_{hetero} \quad \text{(Eq. 25)}$$

The first component (σ^2_{instr}) represents instrument noise and calibration uncertainties. The second component represents uncertainties caused by the clear-sky radiative transfer (σ_{clear}). σ_{clear} is assumed to decrease linearly with increasing $\boldsymbol{e_c}$. For opaque clouds, the uncertainties associated with clear-sky radiative transfer are assumed to be negligible. Due to the large variation in NWP biases on land and ocean, separate land and ocean uncertainties are assumed. The third component (σ_{hetero}) is the term that accounts for the larger uncertainty of the forward model in regions of large spatial heterogeneity. Currently, the ACHA uses the standard deviation of each element of $\boldsymbol{y}$ computed over a 3x3 pixel array as the value of σ_{hetero}. Table 3 provides the current values used for the instrumental and clear-sky terms in constructing $\boldsymbol{S_y}$.

Table 3: The a priori *(first guess) retrieval values used in the ACHA retrieval.*

Cloud Type	**T_c**	**$\sigma(T_c)$**	**τ_{14}**	**σ(ε)**	**β**	**σ(β)**
Spare/Fog	BT(11μm)	10 K	1.2	0.4	1.3	0.2
Liquid Water	BT(11μm)	10 K	2.3	0.2	1.3	0.2

Supercooled Liquid Water	BT(11µm)	10 K	2.3	0.2	1.3	0.2
Mixed Phase	BT(11µm)	10 K	2.3	0.2	1.3	0.2
Optically Thick Ice	BT(11µm)	10 K	2.3	0.2	1.1	0.2
Optically Thin Ice /Cirrus	T(tropo)-15K	20 K	0.9	0.4	1.1	0.2
Multi-layer Ice	T(tropo)-15K	20 K	2.0	0.4	1.1	0.2

Where the apriori value of the 11 micron emissivity, $\varepsilon_{c,ap}(11\mu m)$, is calculated as follows

$$\varepsilon_{c,ap}(11\mu m) = 1 - \exp\left(-\tau_{14} / \cos\left(sat\_zen\right)\right)$$

1.11.2.3 Estimation of Quality Flags and Errors

One of the benefits of the 1DVAR approach is the diagnostic terms it generates automatically. If the values of $\boldsymbol{S_a}$, $\boldsymbol{S_y}$ and $\boldsymbol{K}$ are properly constructed, the values of $\boldsymbol{S_x}$ should provide an estimate of the uncertainties of the retrieved parameters, $\boldsymbol{x}$. The diagonal term of $\boldsymbol{S_x}$ provides the uncertainty expressed as a variance of each parameter. While these estimates are useful, the current ACHA also generates a 4-level quality flag. The integer quality flags are determined by the relative values of the diagonal terms of $\boldsymbol{S_x}$ and $\boldsymbol{S_a}$. The assignment of the parameter quality indicator is shown in the table below

Flag value	**Description**
0	Retrieval did not converge
1	$S_x[i,i] \geq S_a[i,i] \times 0.444$
2	$S_a[i,i] \times 0.444 > S_x[i,i] \geq S_a[i,i] \times 0.111$
3	$S_a[i,i] \times 0.111 > S_x[i,i]$

1.11.2.4 Impact of Local Radiative Center Pixels

As discussed above, the first pass through the retrieval occurs for those pixels determined to be local radiative centers which physically correspond to local maxima in cloud opacity. The full pixel processing order is described below. The objective is to first apply the retrieval to the more opaque pixels and to use this information for the less opaque pixels. In the ACHA, the *a priori* value of $\boldsymbol{T_c}$ for pixels that have local radiative centers identified for them are assumed to be the values of $\boldsymbol{T_c}$ estimated for the local radiative centers. The uncertainty of the *a priori* $\boldsymbol{T_c}$ values remain those given in Table 4.

Table 4: Values of uncertainty for the forward model used in the ACHA retrieval.

Element of *f*	σ_{instr}	σ_{clear} **(Ocean)**	σ_{clear} **(Land)**
T(11um)	1.0	1.5	5.0

BTD(11 – 12μm)	1.0	0.5	1.0
BTD(11 – 13μm)	2.0	4.0	4.0

1.11.2.5 Treatment of Multi-layer Clouds

For pixels determined to be multi-layer clouds, the lower boundary condition is assumed to be a lower cloud and not the surface of the earth. With this assumption, the forward model remains unchanged when treating multi-layer clouds. As discussed by Heidinger and Pavolonis (2009), the mean height of water clouds determined from MODIS is 2 km above the surface. Therefore, for all multi-layer pixels, the lower boundary condition is assumed to be an opaque cloud situated 2 km above the surface of the earth. The same equations apply except that the clear-sky observations are recomputed to reflect the change in the lower boundary condition. It is a goal for future versions of this algorithm to dynamically compute the height/temperature of the lower cloud layer in multi-layer situations.

In the ACHA, information about the height of the surrounding low clouds is used to estimate the height of low clouds underneath higher clouds in detected multi-layer situations. Figure 9 provides a visual aid for understanding this process. In this example, assume that the ABI pixel observed above Low Cloud #3 is correctly identified as a multi-layer cloud by the ABI cloud typing algorithm. Also, assume that Low Clouds #1 and #5 are correctly identified as low clouds and have successful cloud height solutions from the ACHA. The ACHA uses the height information for Low Clouds #1 and #5 to estimate the height of Low Cloud #3 instead of assuming a fixed height of all low clouds detected below high clouds. This computation is accomplished by taking the mean of all low cloud pressures that surround the multi-layer cloud pixel within an *NxN* box, where $N=2*d_x+1$. Currently, the search radius, d_x, of the box is set to 5. Thus, This variable is a configurable parameter (INTERP_LOWER_CLOUD_PIXEL_RADIUS). If the *NxN* box does not fit within the extents of the array (ex. the edges of the current segment), then only the available values will be used in the computation of the mean low cloud pressures. If no low cloud results are found within the *NxN* box, a default value of the cloud pressure is used. This default value is 200 hPa lower than the surface pressure. The application of this logic requires that the low cloud information be available before processing the multi-layer pixels. This logic is described in the next section.

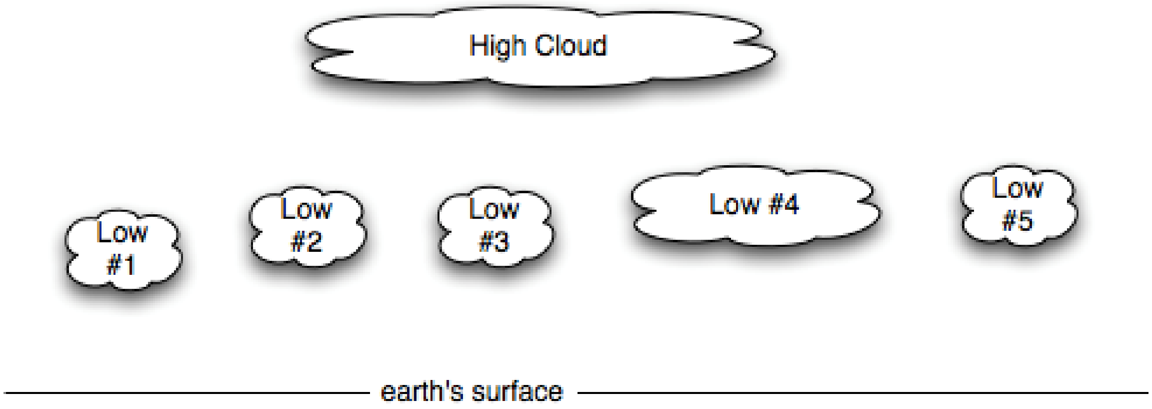

Figure 9 Schematic illustration of multi-layer clouds.

1.11.2.6 Pixel Processing Order with the ACHA

As stated above, applying the multi-layer logic and applying local-radiative center logic require that some pixels be processed before others. In this section, we describe this logic. The pixel processing order in the ACHA is as follows:

1. Single-layer Radiative Centers,
2. Non-local radiative center water clouds,
3. Multi-layer clouds, and
4. All remaining unprocessed cloudy pixels.

Pixels that are single-layer radiative centers can be done first since they rely on the results of now other pixels. Pixels that are single-layer water clouds can then be processed because they would be influenced by the pixels that are single layers and radiative centers. Single-layer ice pixels cannot be processed yet since they may require knowledge of the multi-layer results if their LRC computation points to a multi-layer pixel. The next pixels that can be processed are the multi-layer pixels. After this computation, all remaining pixels can be processed.

1.11.2.7 Computation of Cloud Height and Cloud Pressure

Once T_c is computed, the NWP temperature profiles are used to interpolate the values of cloud-top pressure, P_c, and cloud-top height, Z_c. At this point simple linear interpolation is used to estimate cloud-top pressure and height, and is performed by the “Profile lookup using temperature”, described in the GOES-R AIADD, utilizing T_c as the input to the function. The returned height, pressure, profile index and weight are constrained at both edges of the profile, as described below:

1. First the NWP level is constrained to the minimum on the number of profiles -1 or the maximum of the returned level index or the tropopause level.
2. If T_c is greater than the temperature at the lowest level of the temperature profile used (which is the tropopause -> surface), and the constrained NWP index

(described above) is equal to the lowest level returned by the profile look up (i.e. number of profiles – 1), then Z_c and P_c are set to the surface height and surface pressure respectively

3. If T_c is less than temperature at the tropopause in the temperature profile, then set P_c to the pressure at the tropopause. This is because the "Profile lookup using Temperature" has logic for heights above the tropopause
4. The final constraints are on Z_c and P_c to restrict them to be above the surface. Z_c is set to 0.0 or Z_c, whichever is larger. Similarly, P_c is set to the surface pressure or P_c, whichever is smaller.

If no inversions are present for the current pixel, the values of Z_c,T_c and P_c are output. An inversion is simply defined as a region in the atmosphere where the temperature increases with height. Figure 10 provides an illustration of an inversion. In the presence of inversions, the monotonic relationship between temperature and pressure/height disappears and a single value of cloud temperature can correspond to multiple pressure or height values. Atmospheric inversions are common at low levels over the ocean. This issue plagues all infrared cloud height algorithms including those employed by the MODIS and GOES sounder teams.

The presence of low-level inversions is determined by the full 101-level inversion level profile from NWP determined as described in the GOES-R AIADD, which is produced from an analysis of temperature profile. Currently, if any layer below 700 hPa and 50 hPa above the surface is found to be warmer than the layer below it, the clouds are assumed to reside in an inversion as illustrated in Figure 10. The layer of the 700 hPa and (Surface Pressure – 50hPa) levels is determined by using the "Profile lookup using Pressure" and using 700 or (Surface pressure – 50hPa) as inputs to the routine, with their respective levels being returned. Should the pixel have a cloud type of "Water", "Supercooled" or "Mixed" and have a surface type of "water", the NWP inversion flag profile is checked between the 700 hPa and (Surface Pressure – 50hPa) levels. If there is an inversion present, the cloud height is estimated by dividing the difference between the cloud temperature and the surface temperature by a predefined lapse rate. In addition the low-level inversion flag (an intermediate product used by the AMV team) is set to "true" for that particular pixel. Currently, the lapse rate is assumed to be the dry adiabatic value of -9.8 K/ km. The vertical resolution of NWP profiles is not sufficient to use them directly in the presence of inversions. The cloud pressure is recomputed utilizing the "Profile lookup using height" routine, described in the GOES-R AIADD, with the recomputed cloud height as the input. The only output that is used from the profile lookup is the returned pressure. All other outputs of the profile lookup are not used.

It is important to note that this issue requires further study. The Cloud Application Team is working with the AMV team and other cloud remote sensing groups to determine an optimal strategy when inversions are present.

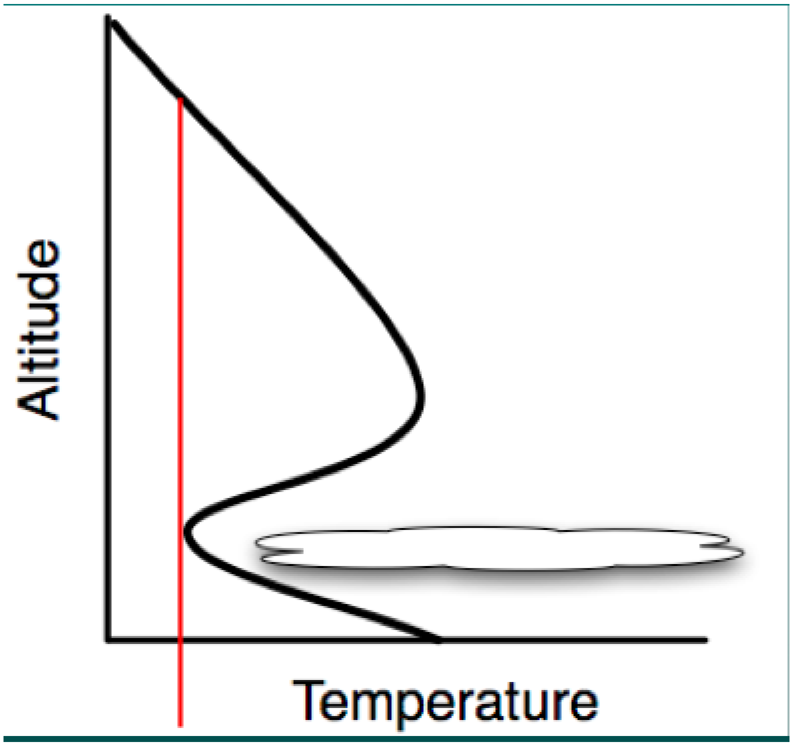

Figure 10 Illustration of a cloud located in a temperature inversion. (Figure provided by Bob Holz of UW/SSEC).

1.11.2.8 Computation of Cloud Layer

Another function of the ACHA is to compute the cloud layer for each cloudy pixel. Currently, we classify each pixel into one of three layers (high, middle and low-level). Using the ISCCP definition, we classify clouds with Pc < 440 hPa as being in the high layer and clouds with Pc > 680 hPa as being low level. Clouds between 440 and 680 hPa are classified as mid level. Subsequent processing is done to take the cloud layer information and generate a cloud cover of each layer.

1.11.3 Algorithm Output

1.11.3.1 Output

The output of the ACHA provides the following ABI cloud products listed in the F&PS:

- Cloud-top temperature,
- Cloud-top pressure,
- Cloud-top height, and
- Cloud cover layer.

Product Cloud Top Temperature is derived at the pixel level for all cloudy pixels.

For products Cloud Top Pressure, Cloud Top Height and Cloud Cover Layers that have a 10 km horizontal resolution, the good quality pixels are averaged over a 5 by 5 pixel block to produce the 10 km resolution Full Disk and CONUS products. For the 4 km mesoscale Cloud top Height and Cloud Cover Layers, the good quality pixels are averaged over a 2 by 2 pixel block to produce the 4 km resolution data. Where the products have a 60 minute refresh, therefore they should be run once an hour.

Example images of the above products are provided in Section 4.2.

1.11.3.2 Intermediate data

The ACHA derives the following intermediate products that are not included in F&PS, but are used in other algorithms, such as the atmospheric motion vector (AMV) algorithm:

- Error estimates,
- Low level inversion flag,
- Cloud 11 μm emissivity, and
- Cloud microphysical index (β).
- Parameter Quality Indicator

The Parameter Quality Indicator is a discretized and normalized version of the error estimates. It is not a substitute for the product quality flag (see below). A detailed description of the parameter quality indicator is provided in section 3.4.2.3.

1.11.3.3 Product Quality Flag

In addition to the algorithm output, a pixel level product quality flag will be assigned. The possible values are as follows:

Flag Value	Description
0	Valid, good quality converged retrieval
1	Invalid pixel due to space view
2	Invalid pixel due to being outside of sensor zenith range
3	Invalid earth pixel due to bad data (bad or missing 11 μm BT or bad/missing clear sky 11 μm BT)
4	Invalid due to cloud mask being clear or probably clear
5	Invalid due to missing cloud type
6	Failed retrieval

1.11.3.4 Processing Information Flag

In addition to the algorithm output and quality flags, processing information, or how the algorithm was processed, will be output for each pixel. If the bit is 0, then the answer was no, and if the bit is 1, the answer is yes.

Bit	Description
0	Cloud Height Attempted
1	Bias Correction Employed
2	Ice cloud retrieval
3	Local Radiative Center Processing Used
4	Multi-layer Retrieval

5	Lower Cloud Interpolation used
6	Boundary Layer Inversion Assumed

1.11.3.5 Metadata

In addition to the algorithm output, the following will be output to the file as metadata for each file:

- Mean, Min, Max and standard deviation of cloud top temperature;
- Mean, Min, Max and standard deviation of cloud top pressure;
- Mean, Min, Max and standard deviation of cloud top height;
- Number of QA flag values ;
- For each QA flag value, the following information is required:
    - Number of retrievals with the QA flag value,
    - Definition of QA flag,
    - Total number of detected cloud pixels, and
    - Terminator mark or determination.

2 Test Datasets and Outputs

2.1 Simulated/Proxy Input Datasets

As described below, the data used to test the ACHA include SEVIRI (imager on MSG) observations collocated with CALIPSO data. Data from August 2006 (summer), February 2007 (winter), April 2007 (spring) and October 2007 (fall) were used to span the entire SEVIRI domain and encompass a full range of conditions.

While SEVIRI does not operate over the GOES domains, we have felt more comfortable using SEVIRI/CALIPSO data than simulated ABI data up to this point. The rest of this section describes the proxy and validation datasets used in assessing the performance of the ACHA. Table 5 shows the channel mapping between the proxy dataset (SEVIRI) and ABI:

Table 5. Channel numbers and wavelengths for the ABI (- planned, but requires additional research from the GOES-RRR program.)*

ABI Channel Number	*SEVIRI Channel Number*	*Wavelength (μm)*
10	6	7.4
13	n/a	10.35
14	9	11.2
15	10	12.3
16	11	13.3

2.1.1 SEVIRI Data

SEVIRI provides 11 spectral channels with a spatial resolution of approximately 3 km and a temporal resolution of 15 minutes. SEVIRI provides the best source of data currently for testing and developing the ACHA. The figure shown below is a full-disk SEVIRI image from 12 Z on August 10, 2006. Except for the 1.38 μm channel, SEVIRI provides an adequate source of proxy data for testing and developing the ACHA. Data from August 2006 (summer), February 2007 (winter), April 2007 (spring) and October 2007 (fall) were used to span the entire SEVIRI domain and encompass a full range of conditions. The SEVIRI data were provided by the UW/SSEC Data Center and processed for the datasets specified in section 4.1.

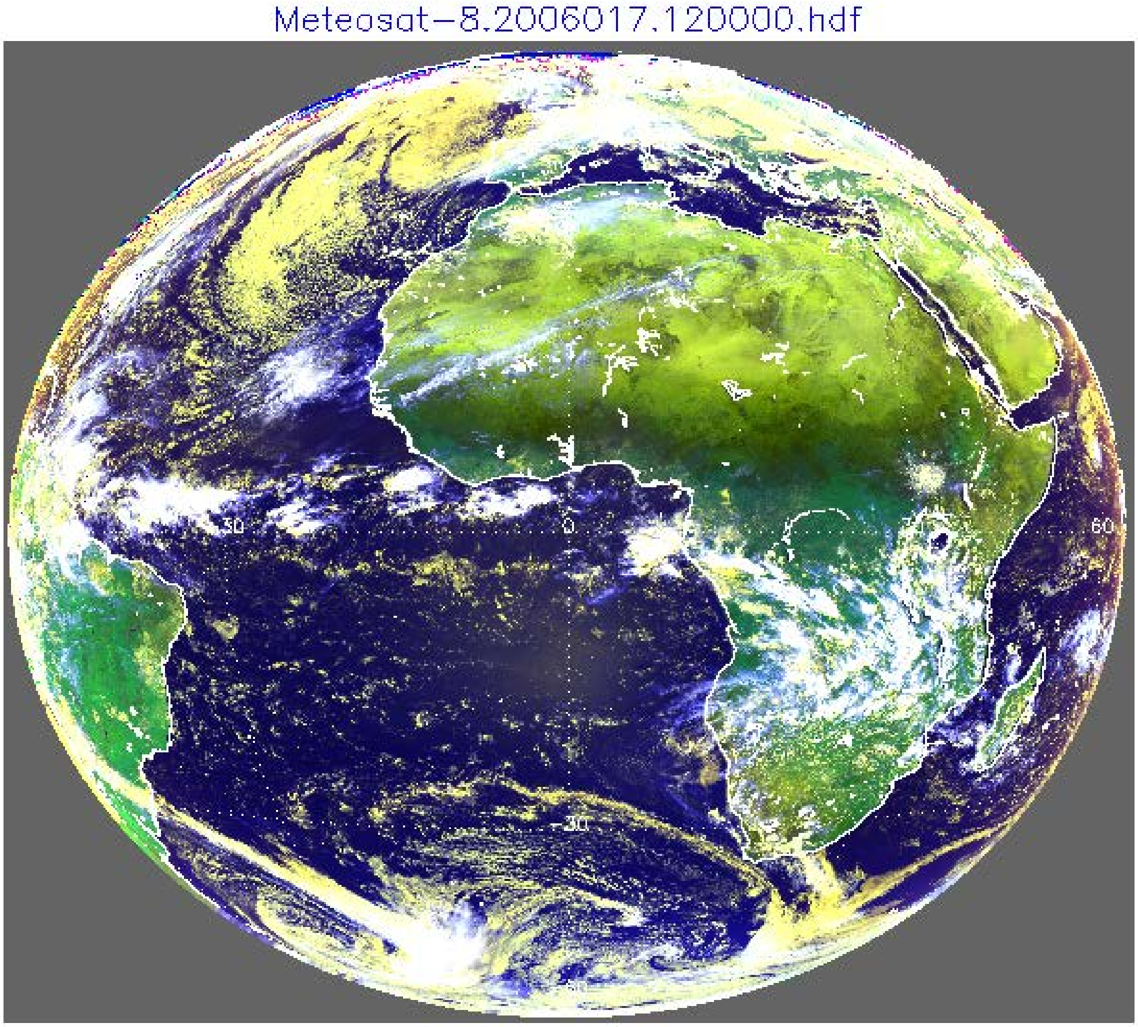

Figure 11 Full disk 0.63, 0.86 and 11 μm false color image from SEVIRI for 12 UTC on January 17, 2006.

2.1.1.1 CALIPSO Data

With the launch of CALIPSO and CloudSat into the NASA EOS A-Train in April 2006, the ability to conduct global satellite cloud product validation increased significantly. Currently, CALIPSO cloud layer results are being used to validate the cloud height product of the ACHA. The CALIPSO data used here are the 1 km cloud layer results.

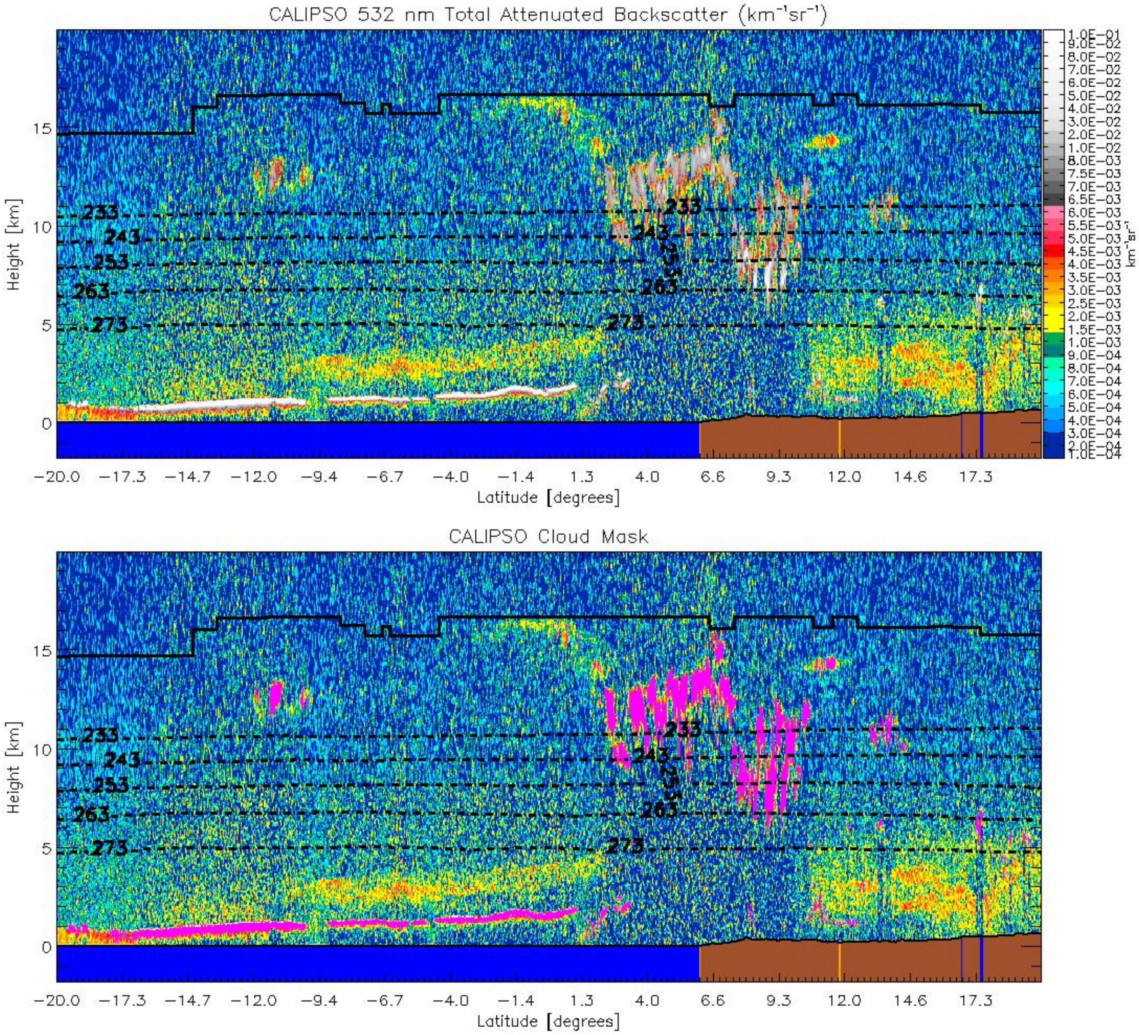

Figure 12 Illustration of CALIPSO data used in this study. Top image shows a 2D backscatter profile. Bottom image shows the detected cloud layers overlaid onto the backscatter image. Cloud layers are colored magenta. (Image courtesy of Michael Pavolonis, NOAA)

2.2 Output from Simulated/Proxy Inputs Datasets

The ACHA result was generated using the SEVIRI data from the dataset specified in section 4.1. During both the TRR and subsequent tests, comparisons between the online and offline (Cloud AWG) output of the ACHA, when the same inputs were used, showed an exact match of the height, temperature and pressure outputs. These tests were conducted under different conditions using the same input for both the online and offline tests. The figures shown below illustrate the ACHA cloud-top temperature, height, pressure, cloud layer and cloud emissivity. These images correspond to 12 Z on January 17, 2006 and correspond to the false-color image shown above. This day was chosen since it was also used in a recent EUMETSAT SEVIRI cloud product comparison workshop.

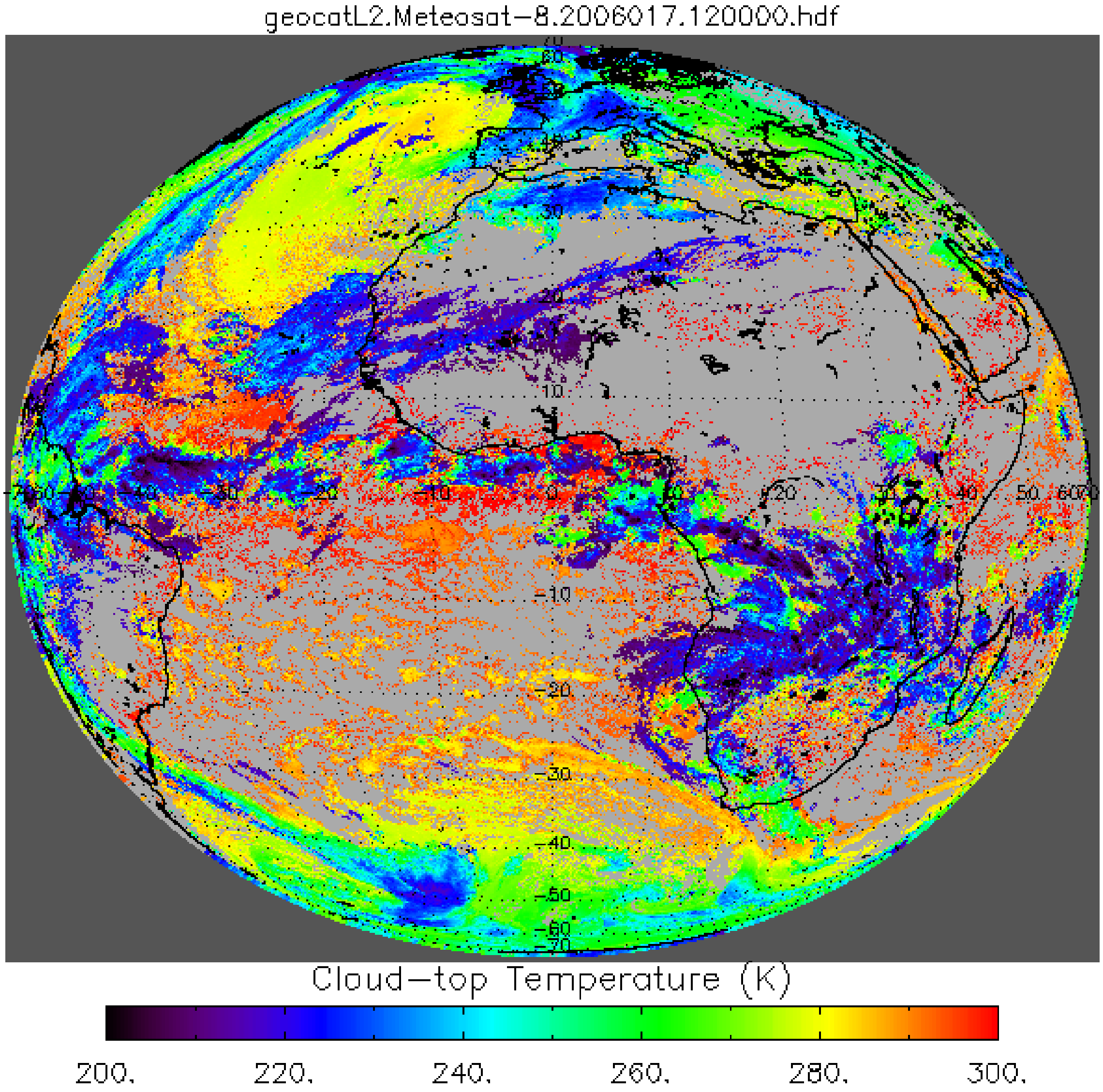
geocatL2.Meteosat-8.2006017.120000.hdf
70
60
40
30
20
10
0
-10
-20
-30
-40
-50
-60
-70
-70
-60
-50
-40
-30
-20
-10
0
10
20
30
40
50
60
70
Cloud-top Temperature (K)
200.
220.
240.
260.
280.
300.

Figure 13 Example ACHA output of cloud-top temperature derived from SEVIRI proxy data for January 17, 2006.

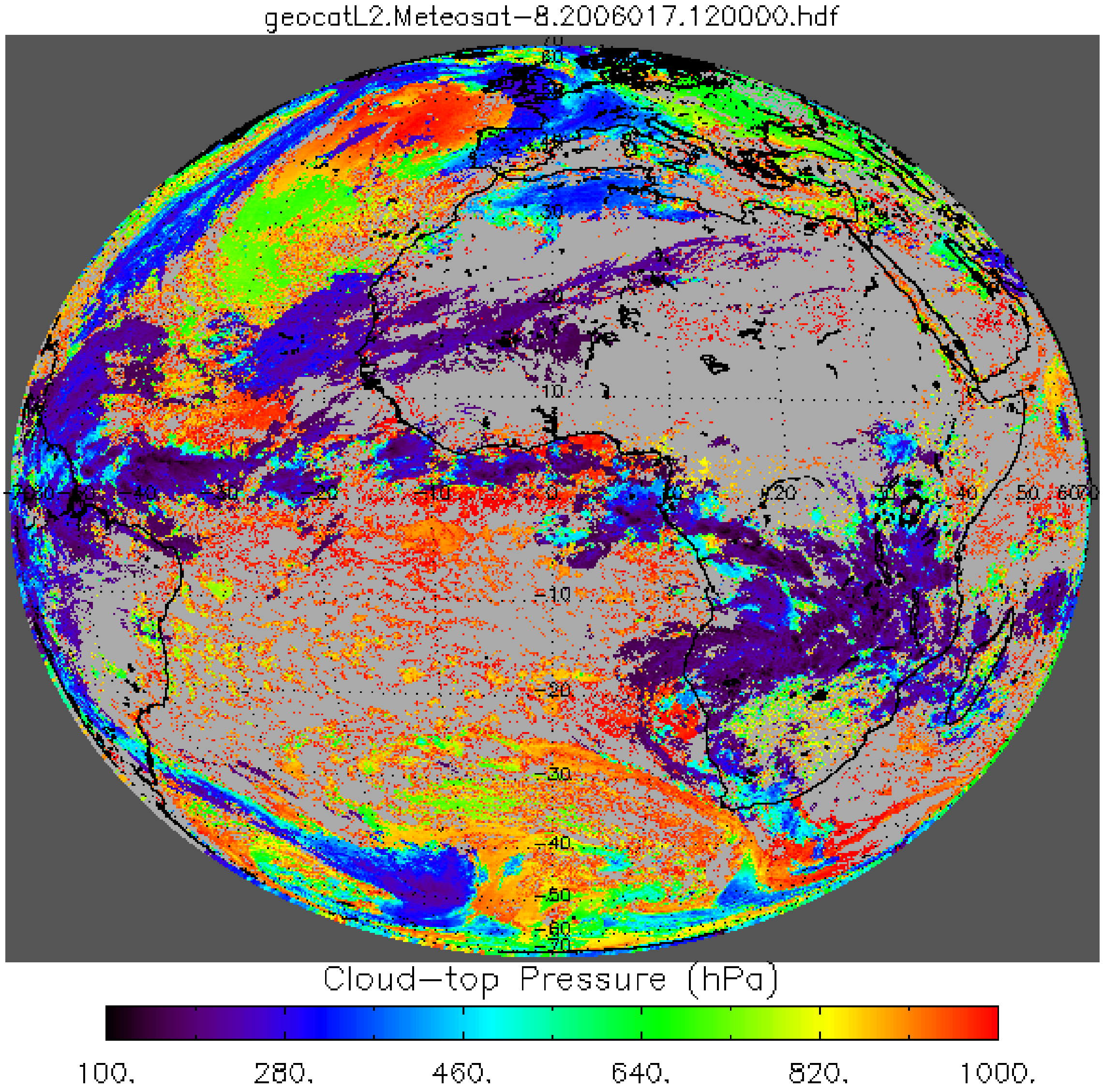
geocatL2.Meteosat-8.2006017.120000.hdf
Cloud-top Pressure (hPa)
100.
280.
460.
640.
820.
1000.

Figure 14 Example ACHA output of cloud-top pressure derived from SEVIRI proxy data for January 17, 2006.

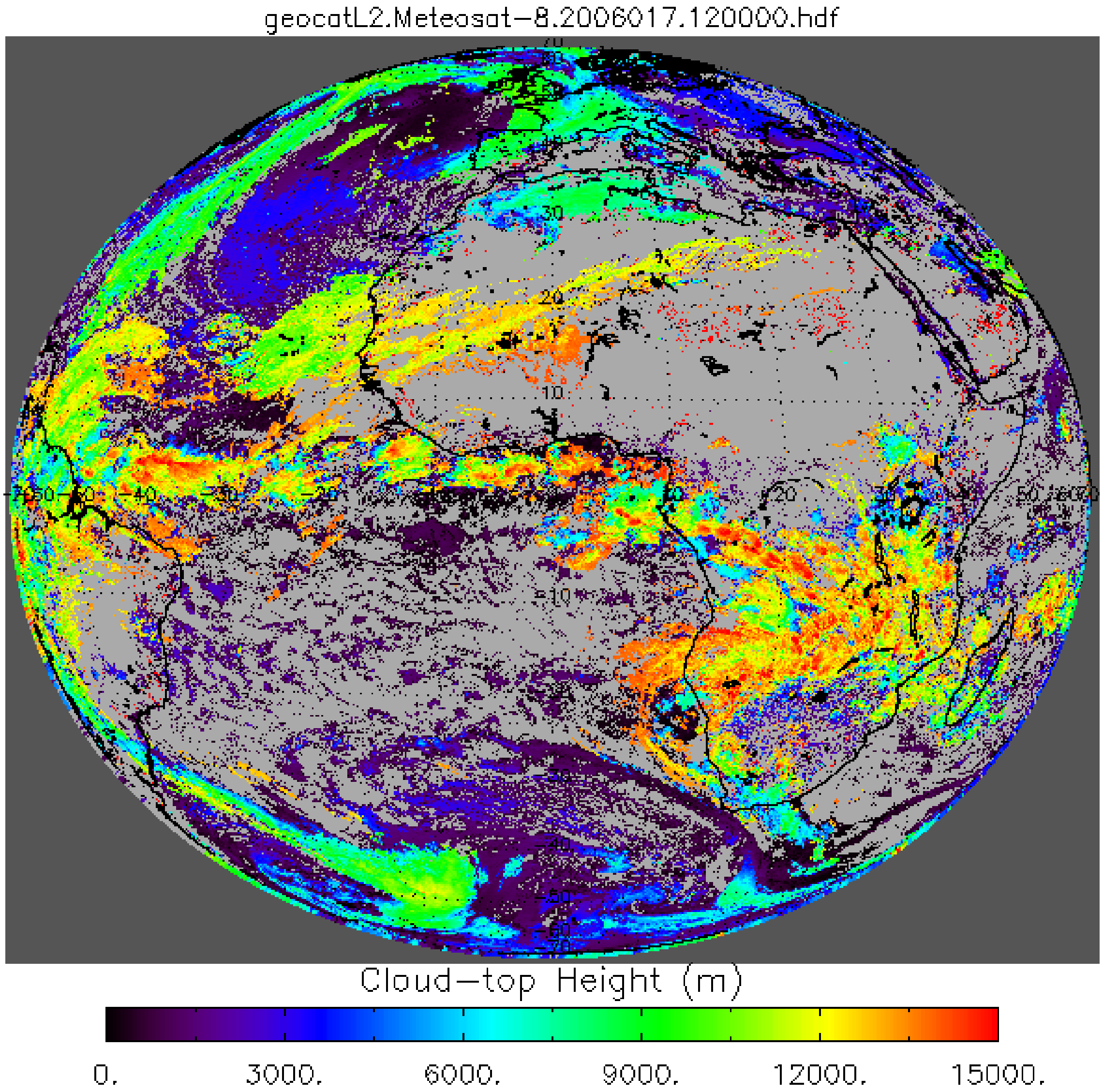
geocatL2.Meteosat-8.2006017.120000.hdf
70
60
50
40
30
20
10
-10
-20
-30
-40
-50
-60
-70
-60
-50
-40
-30
-20
-10
10
20
30
40
50
60
Cloud-top Height (m)
0.
3000.
6000.
9000.
12000.
15000.

Figure 15 Example ACHA output of cloud-top height derived from SEVIRI proxy data for January 17, 2006.

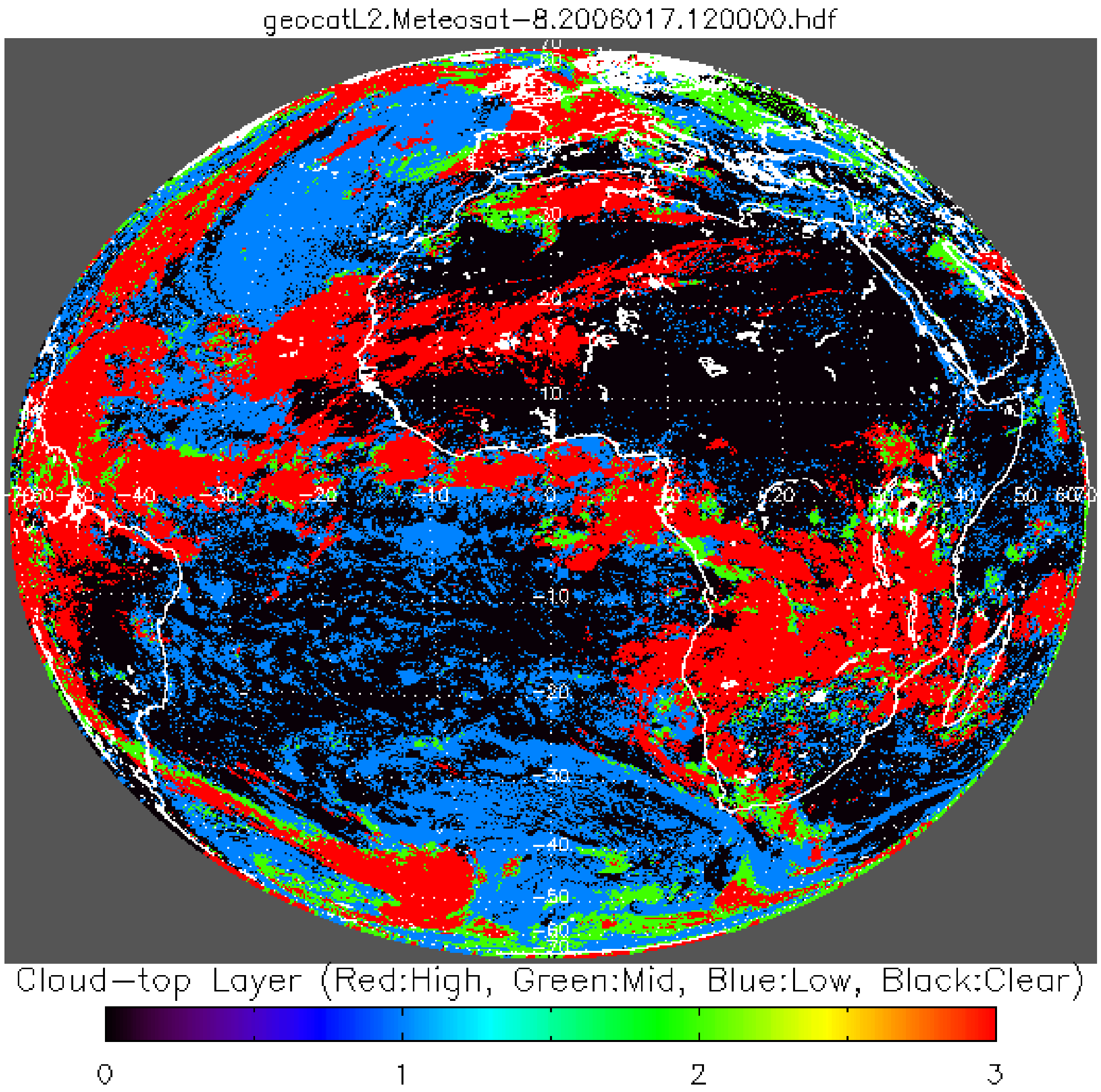
geocatL2.Meteosat-8.2006017.120000.hdf
70
60
50
40
30
20
10
-10
-20
-30
-40
-50
-60
-70
-40
-30
-20
-10
0
20
40
50
Cloud–top Layer (Red:High, Green:Mid, Blue:Low, Black:Clear)
0
1
2
3

Figure 16 Example ACHA output of cloud-top layer derived from SEVIRI proxy data for January 17, 2006.

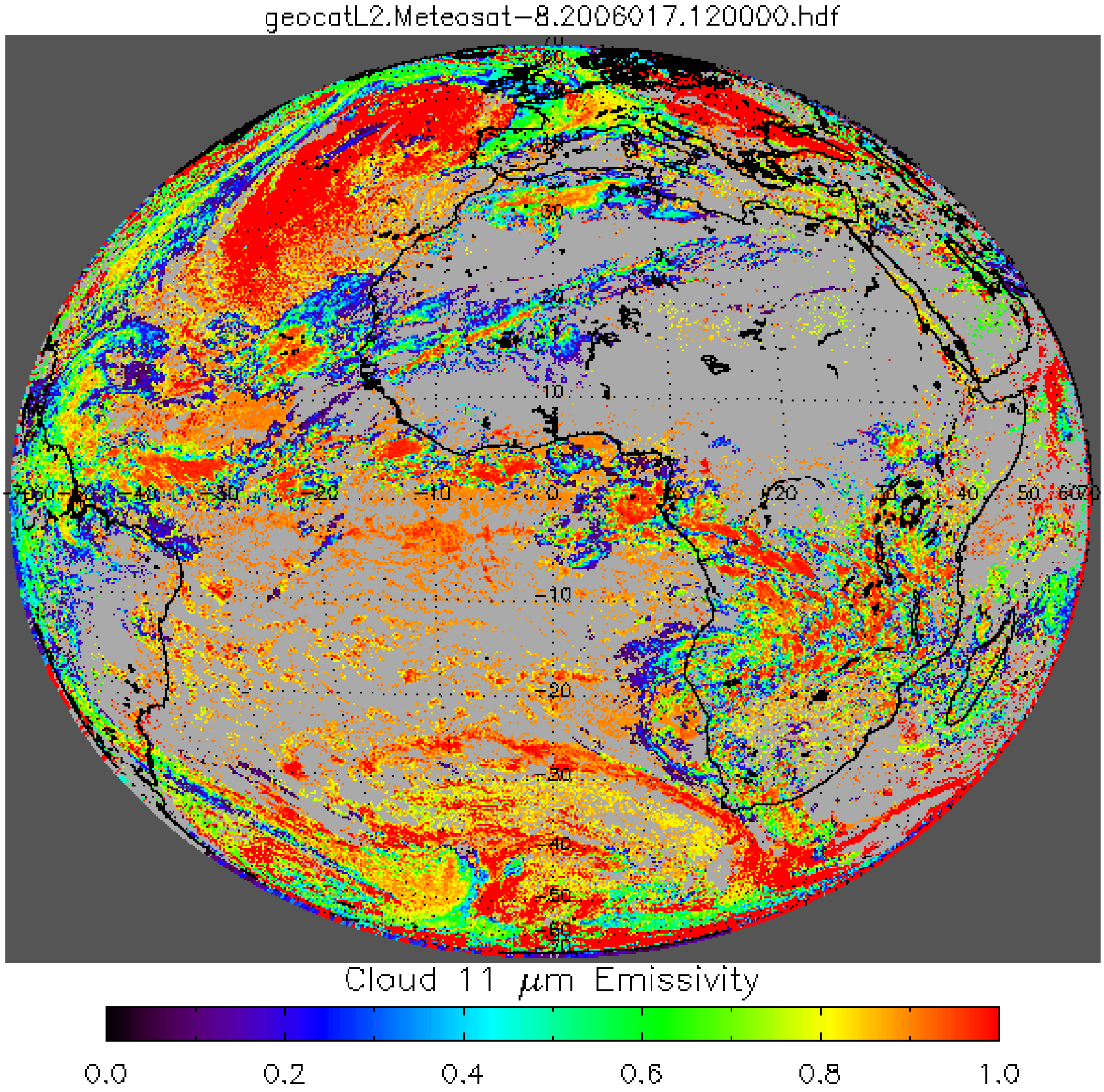
geocatL2.Meteosat-8.2006017.120000.hdf
70
60
50
40
30
20
10
0
-10
-20
-30
-40
-50
-60
-70
-60
-50
-40
-30
-20
-10
20
30
40
50
60
Cloud 11 μm Emissivity
0.0
0.2
0.4
0.6
0.8
1.0

Figure 17 Example ACHA output of the 11µm cloud emissivity derived from SEVIRI proxy data for January 17, 2006

2.2.1 Precisions and Accuracy Estimates

To estimate the precision and accuracy of the ACHA, CALIPSO data from NASA EOS A-Train are used. This new data source provides unprecedented information on a global scale. While surface based sites provide similar information, the limited sampling they offer requires years of analysis to generate the amount of collocated data provided by CALIPSO in a short time period.

2.2.1.1 MODIS Analysis

The MODIS cloud height products (MYD06) have proven to be a useful and accurate source of information to the cloud remote sensing community. The MYD06 cloud height algorithm employs the longwave CO_2 channels in a CO_2 slicing approach to estimate the cloud-top pressure and cloud effective cloud amount. More details on this algorithm are available in the MODIS MYD06 ATBD (Menzel et al., 2006). The MODIS MYD06 ATBD quotes the cloud-top pressure accuracy to be roughly 50 mb, which is under the GOES-R ABI specification of 100 mb.

Given the wide use of the MYD06 product set, a comparison between the ACHA and MYD06 is warranted. While the MYD06 product set does provide the direct measure of cloud height provided by CALIPSO, it does complement the verification by providing qualitative comparisons over a larger domain. Given the availability of the longwave CO_2 channels on MODIS, we expect MYD06 to provide superior results especially for semitransparent cirrus.

To compare the ACHA results to those from MODIS, we analyzed Aqua MODIS data that were nearly coincident with SEVIRI observations. We currently use 3 MODIS granules that provide 15 minutes of data. We then compare these results to SEVIRI data that are closest in time. Our time threshold is 7.5 minutes. Both datasets are remapped to a constant projection with a spatial resolution of 0.08 degrees.

An example of this comparison is shown in Figure 17. In this figure, the top two panels show the MODIS and SEVIRI 0.65 mm reflectance images. The bottom left panel shows the time difference between the MODIS and SEVIRI data. The bottom right image shows the pixels used in this analysis. In addition to the time criteria, additional criteria for inclusion were placed on the agreement between the SEVIRI and MODIS observations.

In this analysis, only pixels where the 11 μm brightness temperatures agreed to within 4K and the 0.65 μm reflectance values agreed to with 5% were used. The rationale for these criteria is that agreement of cloud products is only expected for pixels which have rough agreement in the observations. Any point that has a color (blue, green or red) is one that met the time and observation criteria. It is also assumed that cloud products should only agree when the cloud detection and phase results agree. The green points in Figure 18 are those that met the additional criteria that both cloud masks were set to cloudy. The red pixels in Figure 18 show the subset of points that also agreed on cloud phase. Note in Figure 18 that while the filtering applied here dramatically reduces the number of points used in the analysis, the number of remaining points available for comparison still numbers over 5000 for this scene which, provides adequate sampling of relative performance of the ACHA algorithms compared to the MODIS algorithms.

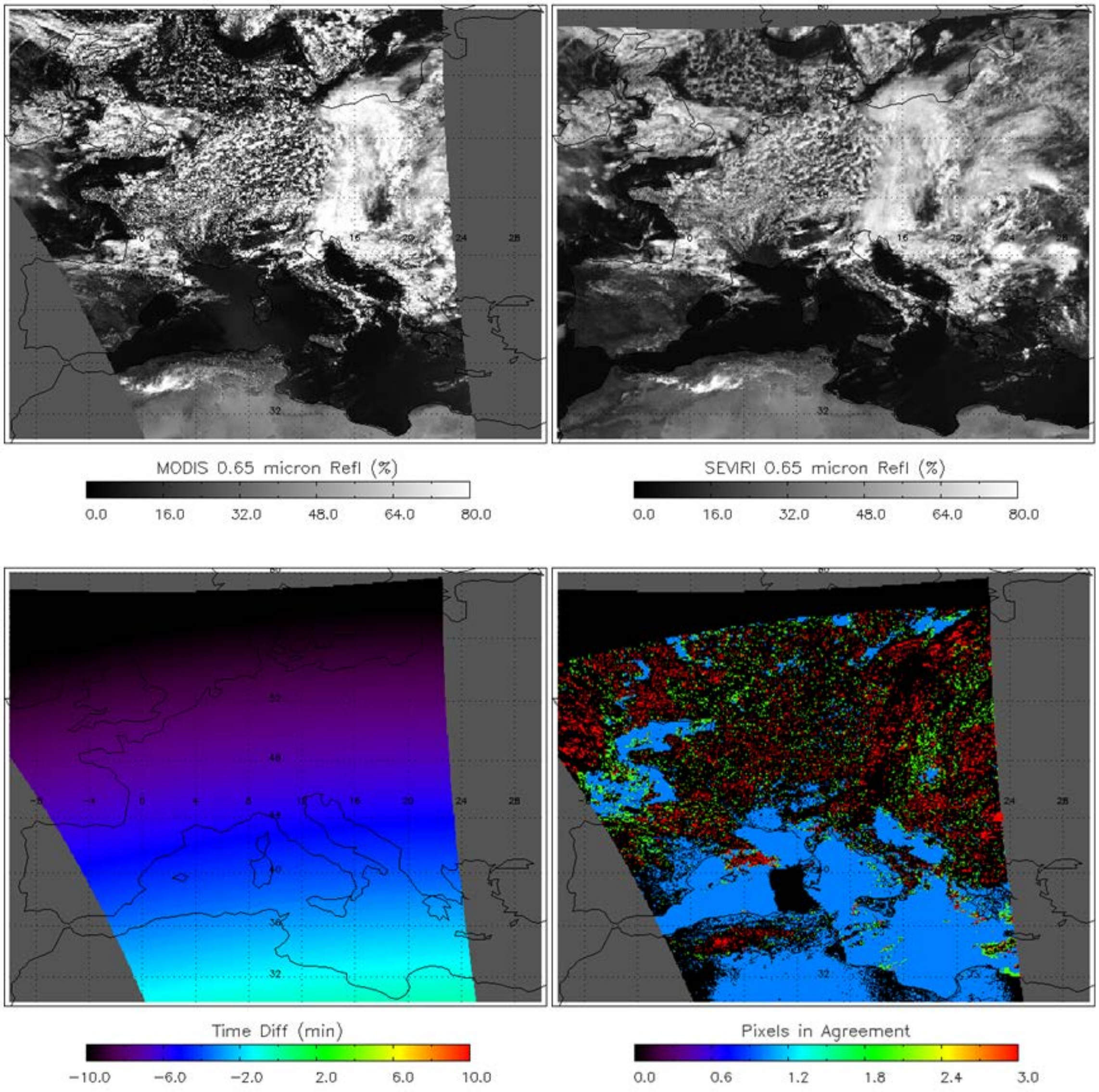
MODIS 0.65 micron Refl (%)
0.0
16.0
32.0
48.0
64.0
80.0
SEVIRI 0.65 micron Refl (%)
0.0
16.0
32.0
48.0
64.0
80.0
Time Diff (min)
−10.0
−6.0
−2.0
2.0
6.0
10.0
Pixels in Agreement
0.0
0.6
1.2
1.8
2.4
3.0

Figure 18 Example images illustrating a comparison of MODIS and SEVIRI data. Image at the top right shows the MODIS 0.65 μm reflectance. Top left image shows the SEVIRI 0.65 μm reflectance. Bottom left image shows the time difference in minutes. Bottom right image shows the pixels used in the analysis. Black colored regions were excluded based on differences in the MODIS and SEVIRI 0.65 μm reflectance and 11 μm brightness temperature. Red, green and blue colored pixels were used in the analysis.

2.2.1.1.1 Comparison of Cloud-top Pressure

Figure 19 shows a comparison of the cloud-top pressure results from those SEVIRI and MODIS points that met all of the criteria described above. No additional filtering on the cloud top pressure values was applied. The results indicate that the MYD06 cloud-top pressures were on average 23.48 hPa lower in the atmosphere than the ACHA results with a standard deviation of 80 hPa. Although comparing two passive satellite measurements cannot be thought of as validation, the bias and precision estimates of the ACHA relative to MODIS indicate the AWG algorithm is performing well.

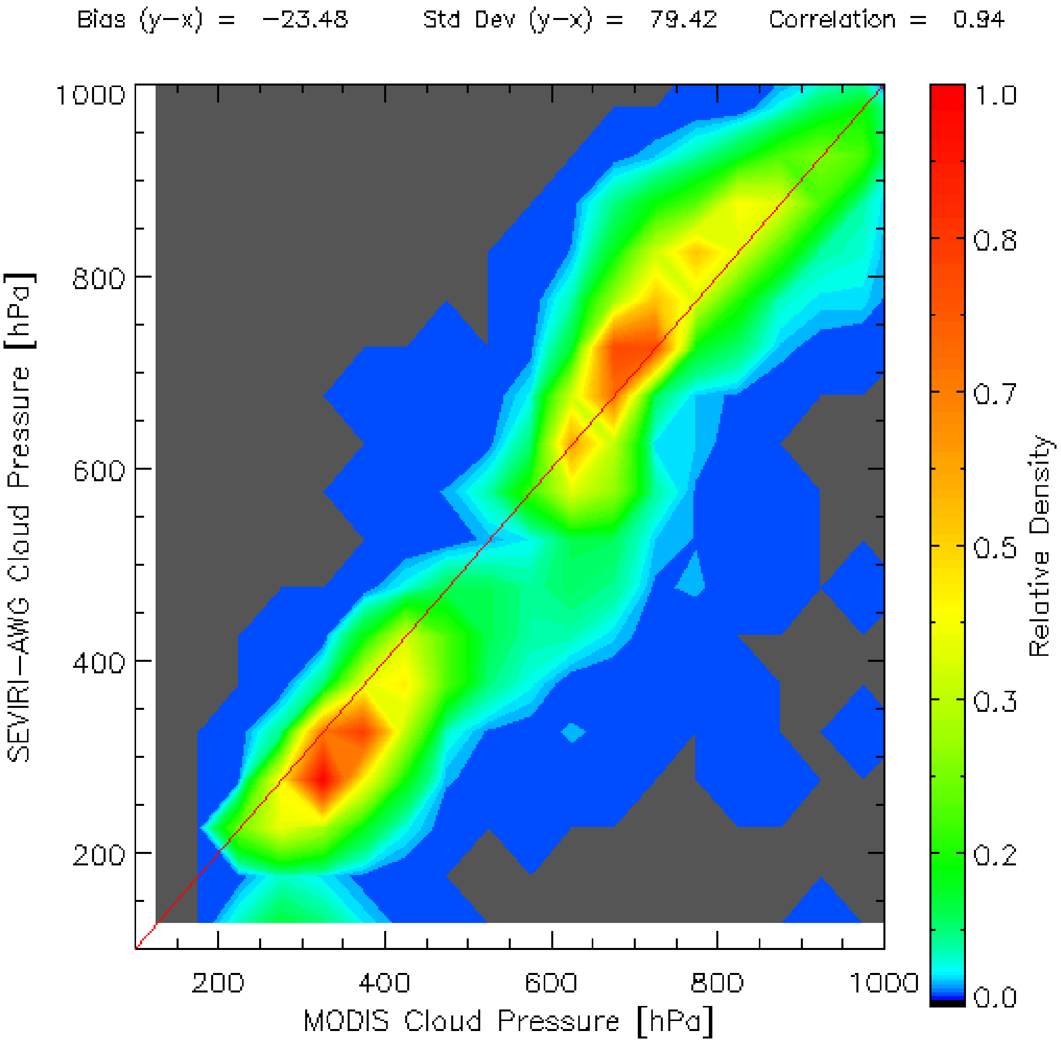

Figure 19 Comparison of cloud-top pressure for June 13, 2008 at 12:15 UTC over Western Europe derived from the MODIS (MYD06) products and from the Cloud Application Team's baseline approach applied to SEVIRI data. Bias (accuracy) and the standard deviation (precision) of the comparison are shown in the figure.

2.2.1.1.2 Comparison of Cloud-top Temperature

An analogous comparison to that shown in Figure 19 constructed for cloud-top temperature is shown in Figure 20. As was the case for cloud-top pressure, the cloud-top temperature comparison shows that the ACHA algorithm applied to SEVIRI is meeting specification relative to MODIS for this scene.

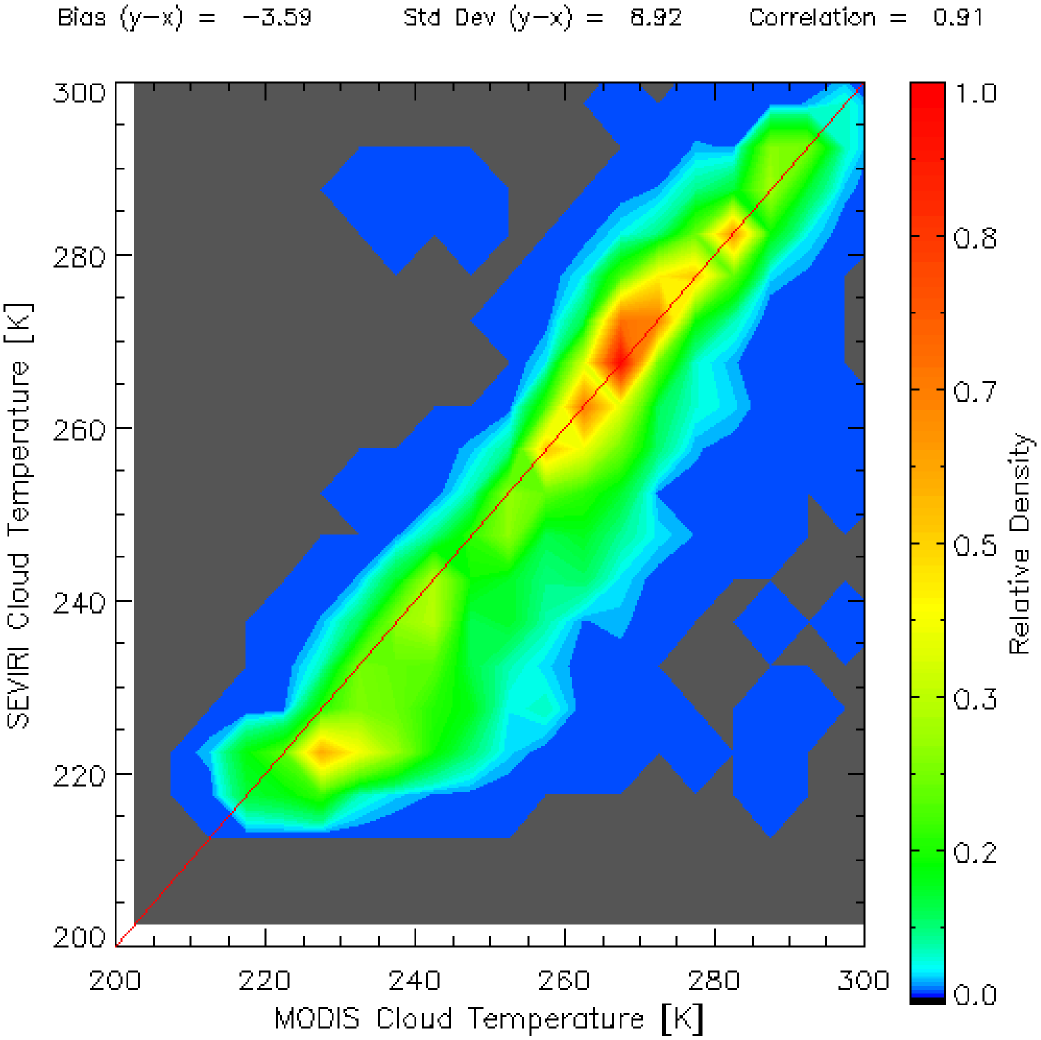

Figure 20 Comparison of cloud-top temperature for June 13, 2008 at 12:15 UTC over Western Europe derived from the MODIS (MYD06) products and from the Cloud Application Team's baseline approach applied to SEVIRI data. Bias (accuracy) and the standard deviation (precision) of the comparison are shown in the figure.

2.2.1.2 CALIPSO Analysis

The CALIPSO/CALIOP data (hereafter referred to as CALIPSO) provide unique information on the cloud vertical structure that can be used to validate the ACHA. For this analysis, a collocation tool has been developed to determine the relevant information provided by CALIPSO for each collocated SEVIRI pixel. This tool has been applied to all SEVIRI data for the datasets specified in section 4.1. For each SEVIRI pixel that is collocated with CALIPSO data, the following information is available:

- Time difference between SEVIRI and CALIPSO,
- Number of cloud layers observed by CALIPSO,
- Cloud-top height of highest cloud layer, and
- Cloud-top temperature of highest cloud layer

In addition to the above information, the SEVIRI 11 μm radiances and the computed clear-sky radiances are used to estimate the cloud emissivity assuming the cloud existed at the height given by CALIPSO. The analysis done spanned data from August 2006 (summer), February 2007 (winter), April 2007 (spring) and October 2007 (fall) over the entire SEVIRI domain and encompassed the full range of conditions. The analysis shown in this section proves the performance of the ACHA based on the cloud height and cloud emissivity as derived from CALIPSO. The height bins were set to a width of 1 km thick and range from 0 to 20 km. The cloud emissivity bins were set to a width of 0.1 and range from -0.2 and 1.2. Emissivities less than 0 imply the observed radiance was less than the clear-sky radiance and emissivities greater than 1.0 imply that the observed radiance was greater than the blackbody emission at the CALIPSO cloud temperature. Only data that were called cloudy by the GOES-R AWG cloud mask (ACM) and by CALIPSO were included in this analysis. Figure 21 shows the total number of pixels and their distribution in Z_c-e_c space for this analysis. Any cells that are colored grey did not have enough points for analysis.

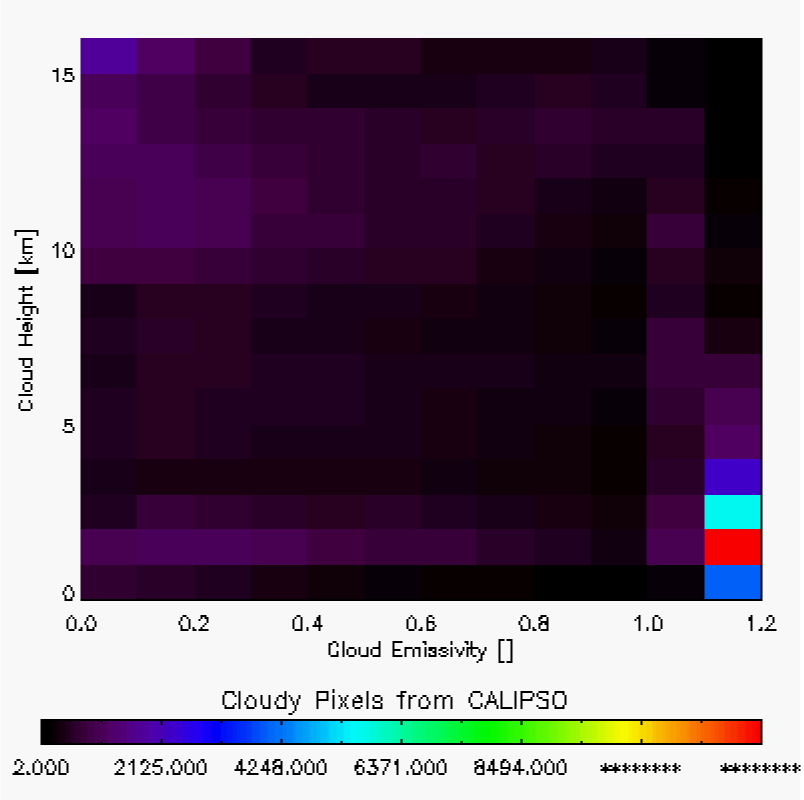

Figure 21 Distribution of points used in the validation of the ACHA applied to SEVIRI data for data observed during simultaneous SEVIRI and CALIPSO periods over eight weeks from four seasons in 2006 and 2007.

2.2.1.2.1   Validation of Cloud Top Height

For each Z_c – e_c bin, the bias in the ACHA – CALIPSO results was compiled. In addition, the standard deviation of the bias (ACHA – CALIPSO) in each bin was also computed. In terms of accuracy and precision, the mean bias is the accuracy and standard deviation of the bias is the precision. The resulting distributions of the mean of the bias and its standard deviation are shown in Figures 21-22. The F&PS specification for accuracy is 0.5 km for low-level clouds with $e_c > 0.5$. While the accuracy is well below this value for the stated cloudiness stratification, the precision of the bias approaches this number.

This analysis indicates that the precision in cloud height for low-level clouds with $e_c > 0.5$ is dominated by the handling of low-level temperature inversions. This situation is a problem for all infrared methods and coordination with the GOES-R Winds Team is in progress to optimize our performance for these clouds. The other area of concern is the standard deviation of the bias for optically thin cirrus. Work is being done to improve in this area as well and involves incorporating radiance biases to improve our ability to reproduce the cirrus observations and use of the water vapor channels to increase the sensitivity to cloud height for these clouds.

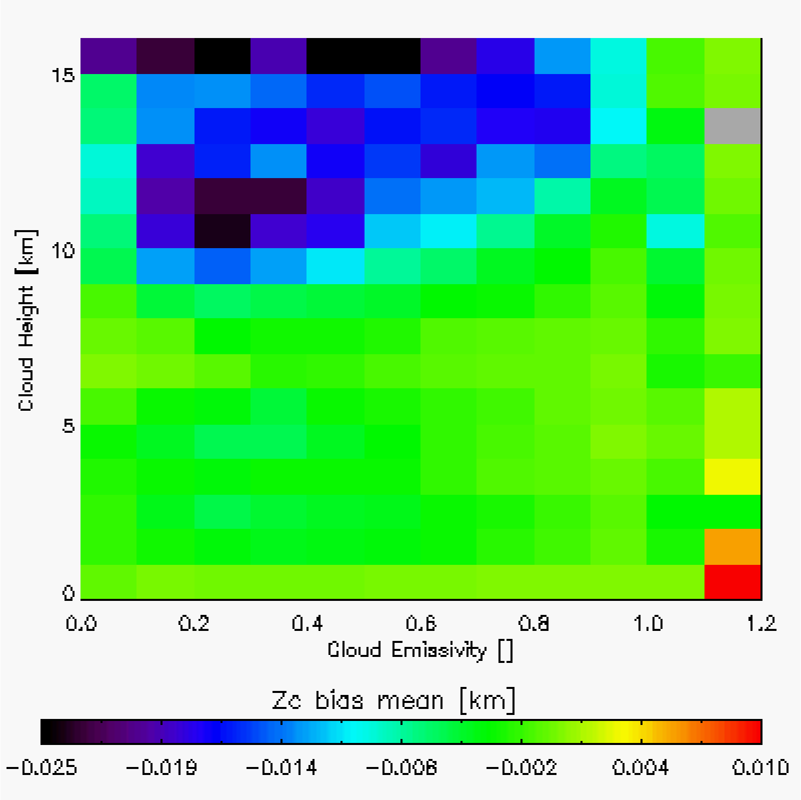

Figure 22 Distribution of cloud-top height mean bias (accuracy) as a function of cloud height and cloud emissivity as derived from CALIPSO data for all SEVIRI observations for four two-week periods covering all seasons. Bias is defined as ACHA – CALIPSO.

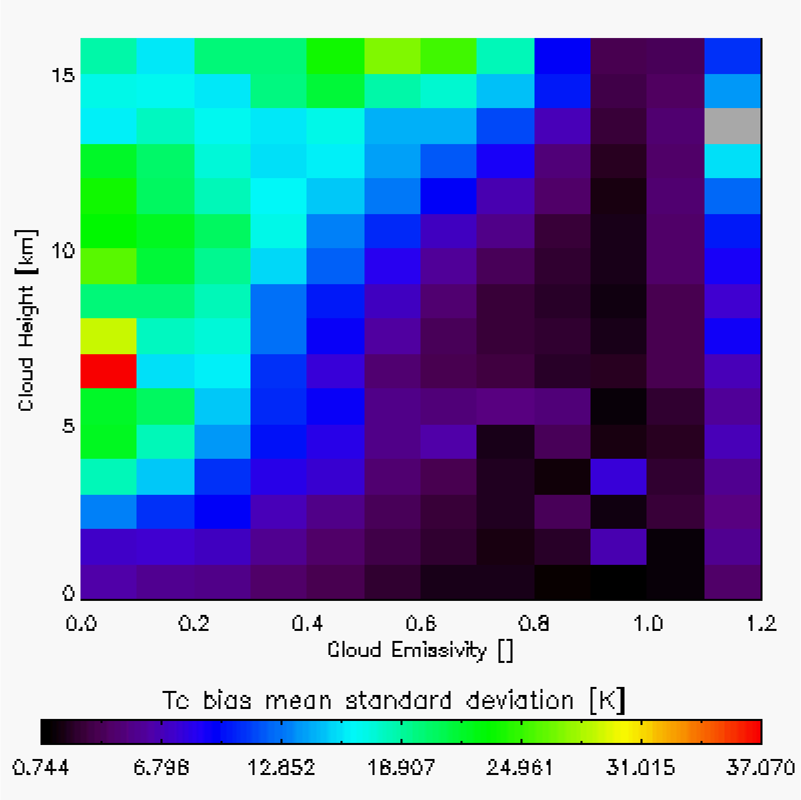

Figure 23 Distribution of cloud-top height of the standard deviation of the bias (precision) as a function of cloud height and cloud emissivity as derived from CALIPSO data for all SEVIRI for four two-week periods covering all seasons. Bias is defined as ACHA – CALIPSO.

2.2.1.2.2 Validation of Cloud Top Temperature

The same analysis was applied to the verification of cloud-top temperature. The resulting mean (accuracy) and standard deviation (precision) of the bias results are shown in Figures 24-25. As expected, the T_c results show the same pattern as the Z_c results. As was the case with the cloud height analysis above, the accuracy of the cloud temperature is very good and meets the F&PS accuracy requirement. As with cloud height, the precision of the cloud temperature results relative to CALIPSO is much worse than the accuracy. The F&PS specification for accuracy for cloud-top temperature is 1 K for purely black-body cloud in a known atmosphere. None of the observed clouds ever meet these restrictions, and therefore the verification of the cloud-top temperature F&PS specification is impossible with real data or realistic simulations.

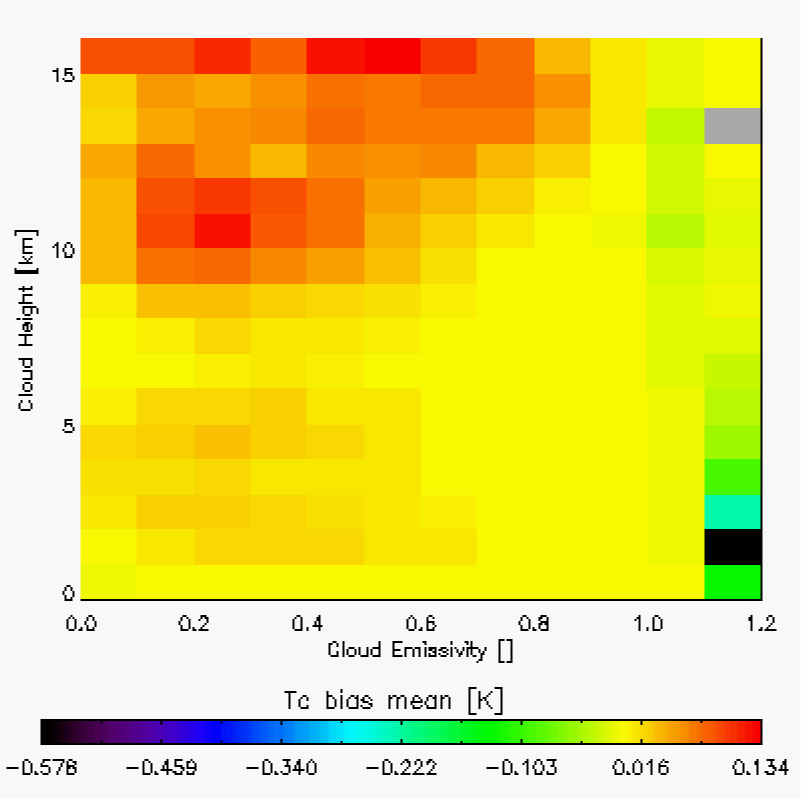

Figure 24 Distribution of cloud-top temperature mean bias (accuracy as a function of cloud height and cloud emissivity as derived from CALIPSO data for all SEVIRI observations for four two-week periods covering all seasons. Bias is defined as ACHA – CALIPSO.

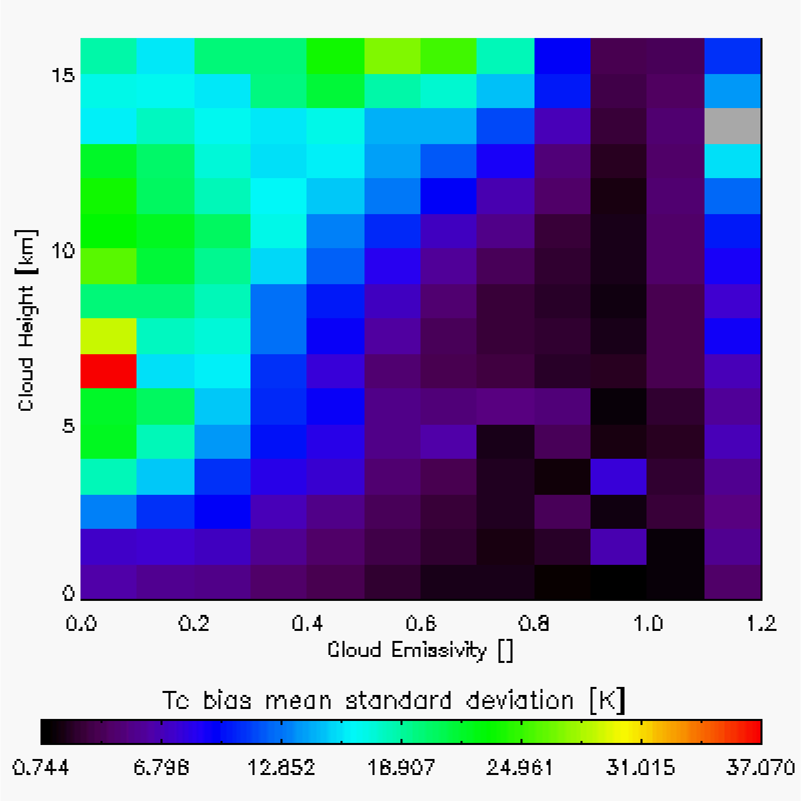

Figure 25 Distribution of cloud-top temperature of the standard deviation of the bias (precision) as a function of cloud height and cloud emissivity as derived from CALIPSO data for all SEVIRI observations for four two-week periods covering all seasons. Bias is defined as ACHA – CALIPSO.

2.2.1.2.3 Validation of Cloud Top Pressure

The current suite of CALIPSO products does not include pressure as a product. We are modifying our tools to estimate cloud pressure from the cloud height products in the CALIPSO product suite. However, the cloud-top pressure errors are highly correlated to the cloud-top height errors shown above. The comparisons to MODIS confirm this correlation.

2.2.1.2.4 Validation of Cloud Layer

The cloud layer product has been defined as a flag that indicates where a cloud-top falls into 3 discrete vertical layers in the atmosphere. These layers are defined as follows:

- Low: pressures between the surface and 680 hPa,
- Mid: pressures between 680 and 44 hPa, and
- High: pressures lower than 440 hPa.

These layers are the standard layers used in many cloud product systems such as those used in the International Satellite Cloud Climatology (ISCCP). Cloud amounts in these layers have often been used for verifying cloud parameterization in NWP forecasts.

As mentioned above, CALIPSO does not generate a standard cloud-top pressure product so direct validation of the cloud layer product using CALIPSO is not possible. However, CALIPSO does generate a product whereby the low layer is defined as clouds with top heights less than 3.25 km, the mid layer is defined as clouds with tops between 3.25 and 6.5 km and the high layer is defined as cloud with tops higher than 6.5 km. These height layers roughly correspond to the pressure layers used to define the ABI product.

Using the CALIPSO layer height definitions, a height-based layer can be derived from the ABI cloud-top heights. In addition, the CALIPSO cloud-top heights of the highest layer can be computed into height-based layer flags. When the CALIPSO and ABI height-based cloud layer flags are compared, a POD value of 91.4 % is computed. The data used in this comparison are the 10-week of SEVIRI runs described above. This level of agreement indicates the ABI cloud layer product meets its accuracy specification of 80%. At this time, there is no precision specification placed on this product.

2.2.2 Error Budget

Using the validation described above, the following table provides our preliminary estimate of an error budget. The "Bias Estimate" column values most closely match our interpretation of the F&PS accuracy specifications. To match the F&PS, these numbers were generated for low-level clouds with emissivities greater than 0.8. Cloud pressure errors were estimated assuming 1000m = 100 hPa which is a good approximation at low levels.

Table 6. Preliminary estimate of error budget for ACHA.

Product	Accuracy Specification (F&PS)	Bias Estimate	Precision Specification (F&PS)	Standard Deviation Estimate
Cloud-top Temperature	4K	-0.22 K	5K	4.75 K
Cloud-top Height	500 m	-0.0002 km	1.5km	0.94 km
Cloud-top Pressure	100 hPa	-0.02 hPa	150 hPa	94 hPa

As Table 6 shows, the ACHA meets the 100% F&PS requirements for precision and accuracy. It is important to identify the three main drivers of the ACHA error budget.

1. *Lack of Knowledge of Low-level Inversions*. The current F&PS specifications demand accurate performance of cloud height for low-level clouds. Even if the instrument and retrievals are perfect and an accurate cloud-top temperature is estimated, the unknown effects of inversions can result in cloud heights failing to meet specification.
2. *Characterization of Channel 16*. Our ability to place cirrus properly is in large part determined by our ability to model the observations within absorption bands (ch16). If poor instrument characterization or manufacture results in unknown spectral response functions, the ability to perform well in the presence of cirrus clouds is in jeopardy.
3. *Multi-layer clouds*. While the AWG cloud type algorithm does include a multi-layer detection, our knowledge of the properties of that lower cloud is limited.

The Cloud Application Team will continue to be involved in developments that impact the above error sources.

3 PRACTICAL CONSIDERATIONS

3.1 Numerical Computation Considerations

The ACHA employs an optimal estimation approach. Therefore, it requires inversions of matrices that can, under severe scenarios, become ill-conditioned. Currently, these events are detected and treated as failed retrievals.

3.2 Programming and Procedural Considerations

The ACHA makes heavy use of clear-sky RTM calculations. The current system computes the clear-sky RTM at low spatial resolution and with enough angular resolution to capture sub-grid variation to path-length changes. This approach is important for latency consideration as the latency requirements could not be met if the clear-sky RTM were computed for each pixel.

3.3 Quality Assessment and Diagnostics

The optimal estimation framework provides automatic diagnostic metrics and estimates of the retrieval error. It is recommended that the optimal estimation covariance matrices be visualized and analyzed on a regular basis. In addition, the CALIPSO analysis described above should be done regularly.

3.4 Exception Handling

The ACHA includes checking the validity of each channel before applying the appropriate test. The ACHA also expects the main processing FRAMEWORK to flag any pixels with missing geolocation or viewing geometry information.

The ACHA does check for conditions where the ACHA cannot be performed. These conditions include saturated channels or missing RTM values. In these cases, the appropriate flag is set to indicate that no cloud temperature, pressure and height are produced for that pixel. In addition, a fill value is stored for the cloud temperature, pressure and height at these pixels.

3.5 Algorithm Validation

It is recommended that the CALIPSO analysis described earlier be adopted as the main validation tool. If CALIPSO type observations are not available, use of surface-based lidars and radars, such as provided by the Atmospheric Radiation Measurement (ARM) program, is recommended.

4 ASSUMPTIONS AND LIMITATIONS

The following sections describe the current limitations and assumptions in the current version of the ACHA.

4.1 Performance

Assumptions have been made in developing and estimating the performance of the ACHA. The following list contains the current assumptions and proposed mitigation strategies.

1. NWP data of comparable or superior quality to the current 6 hourly GFS forecasts are available. (Use longer range GFS forecasts or switch to another NWP source – ECMWF.)
2. RTM calculations are available for each pixel. (Use reduced vertical or spatial resolution in driving the RTM.)
3. All of the static ancillary data are available at the pixel level. (Reduce the spatial resolution of the surface type, land/sea mask and or coast mask.)
4. The processing system allows for processing of multiple pixels at once for use of spatial texture information. (No mitigation possible)

For a given pixel, should any channel not be available, the ACHA algorithm will not be performed on that particular pixel.

4.2 Assumed Sensor Performance

It is assumed that the ABI sensor will meet its current specifications. However, the ACHA will be dependent on the following instrumental characteristic:

- Unknown spectral shifts in some channels will cause biases in the clear-sky RTM calculations that may impact the performance of the ACHA.

4.3 Pre-Planned Product Improvements

While development of the baseline ACHA continues, we expect in the coming years to focus on the issues noted below.

4.3.1 Optimization for Atmospheric Motion Vectors

The AMV team is critically dependant on the performance of this algorithm. In addition, the AMV team has a long heritage of making its own internal estimates of cloud-top height. Therefore, it is important that the CAT and AMV teams work together, particularly on the issue of atmospheric inversions.

4.3.2 Implementation of Channel Bias Corrections

The MYD06 development team has found that bias corrections are critical for the proper use of infrared channels for cloud height estimation. Currently, we utilize no bias corrections in ACHA. In addition, we plan to implement a mechanism to account for the large surface biases in NWP data.

4.3.3 Use of 10.4 μm Channel

The 10.4 μm channel is new to the world of satellite imagers. We expect to incorporate this channel into the ACHA to improve our cloud microphysical retrievals. We expect the GOES-R Risk Reduction projects to demonstrate its use before implementation into the operational algorithm.

5 REFERENCES

Heidinger, A. K.; Pavolonis, M. J.; Holz, R. E.; Baum, Bryan A. and Berthier, S.. **Using CALIPSO to explore the sensitivity to cirrus height in the infrared observations from NPOESS/VIIRS and GOES-R/ABI**. Journal of Geophysical Research, Volume 115, 2010, Doi:10.1029/2009JD012152, 2010

Heidinger, Andrew K. and Pavolonis, Michael J.. **Gazing at cirrus clouds for 25 years through a split window, part 1: Methodology**. Journal of Applied Meteorology and Climatology, Volume 48, Issue 6, 2009, pp.110-1116

Hannon, S. L. L. Strow, and W. W. McMillan, 1996: Atmospheric infrared fast transmittance models: A comparison of two approaches, Proceedings of SPIE, 2830, 94-105.

Hansen, M., R. DeFries, J.R.G. Townshend, and R. Sohlberg (1998), UMD Global Land Cover Classification, 1 Kilometer, 1.0, Department of Geography, University of Maryland, College Park, Maryland, 1981-1994.

W. P. Menzel, R. A. Frey, B. A. Baum, and H. Zhang, “Cloud Top Properties and Cloud Phase - Algorithm Theoretical Basis Document. Products: 06-L2, 08-D3, 08-E3, 08-M3,” NASA Goddard Space Flight Center, Tech. Rep. ATBD Reference Number: ATBD-MOD-05, 2006.

Seemann, S.W., E. E. Borbas, R. O. Knuteson, G. R. Stephenson, H.-L. Huang, 2007: Development of a Global Infrared Land Surface Emissivity Database for Application to Clear Sky Sounding Retrievals from Multi-spectral Satellite Radiance Measurements. Journal of Applied Meteorology and Climatology, Accepted April 2007.

Rodgers, C.D., 1976: Retrieval of atmospheric temperature and composition from remote measurements of thermal radiation. Rev. Geophys. Space Phys., 60, 609-624.

GOES-R Series Ground Segment (GS) Project Functional and Performance Specification (F&PS) [G417-R-FPS-0089]

GOES-R ABI Cloud Mask Algorithm Theoretical Basis Document

GOES-R ABI Cloud Type/Phase Algorithm Theoretical Basis Document

GOES-R Level 1 Requirements Document (L1RD)

GOES-R Series Mission Requirements Document (MRD) [P417-R-MRD-0070]

GOES-R Acronym and Glossary (P417-R-LIST-0142)

Yang, P., H. Wei, H.-L. Huang, B. A. Baum, Y. X. Hu, G. W. Kattawar, M. I. Mishchenko, and Q. Fu, 2005: Scattering and absorption property database for nonspherical ice particles in the near- through far-infrared spectral region, Appl. Opt., 44, 5512–5523.

Appendix 1: Common Ancillary Data Sets

1. NWP_GFS

a. *Data description*

Description: NCEP GFS model data in grib format – 1 x 1 degree (360x181), 26 levels
Filename: gfs.tHHz.pgrbfhh
Where,
HH – Forecast time in hour: 00, 06, 12, 18
hh – Previous hours used to make forecast: 00, 03, 06, 09
Origin: NCEP
Size: 26MB
Static/Dynamic: Dynamic

b. Interpolation description

There are three interpolations are installed:

NWP forecast interpolation from different forecast time:

Load two NWP grib files which are for two different forecast time and interpolate to the satellite time using linear interpolation with time difference.

Suppose:

T1, T2 are NWP forecast time, T is satellite observation time, and T1 < T < T2. Y is any NWP field. Then field Y at satellite observation time T is:

$$Y(T) = Y(T1) * W(T1) + Y(T2) * W(T2)$$

Where W is weight and

$$W(T1) = 1 – (T-T1) / (T2-T1)$$
$$W(T2) = (T-T1) / (T2-T1)$$

NWP forecast spatial interpolation from NWP forecast grid points. This interpolation generates the NWP forecast for the satellite pixel from the NWP forecast grid dataset.

The closest point is used for each satellite pixel:

1) Given NWP forecast grid of large size than satellite grid
2) In Latitude / Longitude space, use the ancillary data closest to the satellite pixel.

NWP forecast profile vertical interpolation

Interpolate NWP GFS profile from 26 pressure levels to 101 pressure levels

For vertical profile interpolation, linear interpolation with Log pressure is used:

Suppose:

y is temperature or water vapor at 26 levels, and y101 is temperature or water vapor at 101 levels. p is any pressure level between p(i) and p(i-1), with $p(i-1) < p < p(i)$. y(i) and y(i-1) are y at pressure level p(i) and p(i-1). Then y101 at pressure p level is:

$$y101(p) = y(i-1) + \log(p[i] / p[i-1]) * (y[i] – y[i-1]) / \log (p[i] / p[i-1])$$

2. SFC_ELEV_GLOBE_1KM

a. *Data description*

Description: Digital surface elevation at 1km resolution.
Filename: GLOBE_1km_digelev.nc
Origin: NGDC
Size: 1843.2 MB
Static/Dynamic: Static

b. *Interpolation description*

The closest point is used for each satellite pixel:

1) Given ancillary grid of large size than satellite grid
2) In Latitude / Longitude space, use the ancillary data closest to the satellite pixel.

3. SFC_TYPE_AVHRR_1KM

a. *Data description*

Description: Surface type mask based on AVHRR at 1km resolution
Filename: gl-latlong-1km-landcover.nc
Origin: University of Maryland
Size: 890 MB
Static/Dynamic: Static

b. *Interpolation description*

The closest point is used for each satellite pixel:

1) Given ancillary grid of large size than satellite grid
2) In Latitude / Longitude space, use the ancillary data closest to the satellite pixel.

4. LRC

a. Data *description*

Description: Local Radiative Center Calculation
Filename: N/A
Origin: NOAA / NESDIS
Size: N/A
Static/Dynamic: N/A

b. Interpolation *description*

It should be first noted that the original description of the local radiative center calculation was done by Michael Pavolonis (NOAA/NESDIS) in section 3.4.2.2 of 80% GOES-R Cloud Type Algorithm Theoretical Basis Document. This description takes several parts of the original text as well as two of the figures from the original text in order to illustrate the gradient filter. In addition, the analysis performed by Michael Pavolonis (NOAA/NESDIS) regarding the number of steps taken is also shown in the LRC description. This description gives an overview and description of how to calculate the local radatitive center. The authors would like to recognize the effort that was done by Michael Pavolonis in the development of this algorithm.

The local radiative center (LRC) is used in various GOES-R AWG algorithms as a measure of where the radiative center for a given cloud is located, allowing for the algorithm to look at the spectral information at an interior pixel within the same cloud while avoiding the spectral information offered by pixels with a very weak cloud radiative signal. A generalized definition of the LRC is that, for a given pixel, it is the pixel location, in the direction of the gradient vector, upon which the gradient reverses or when the input value is greater than or equal to the gradient stop value is found, whichever occurs first.

Overall, this use of spatial information allows for a more spatially and physically consistent product. This concept is also explained in Pavolonis (2010).

The gradient vector points from low to high pixels of the input, such that the vector is perpendicular to isolines of the input value. This concept is best illustrated with a figure. Figure 1, which is of $\square_{stropo}(11\square m)$, is the actual gradient vector field, thinned for the sake of clarity. As can be seen, the vectors in this image point from cloud edge towards the optically thicker interior of the cloud. This allows one to consult the spectral information at an interior pixel within the same cloud in order to avoid using the spectral information offered by pixels with a very weak cloud radiative signal.

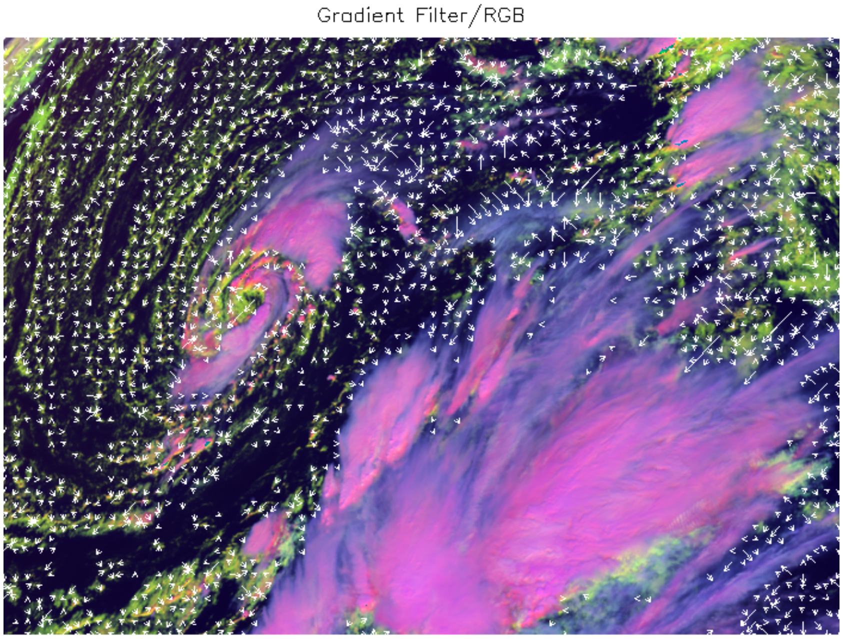

Gradient Filter/RGB

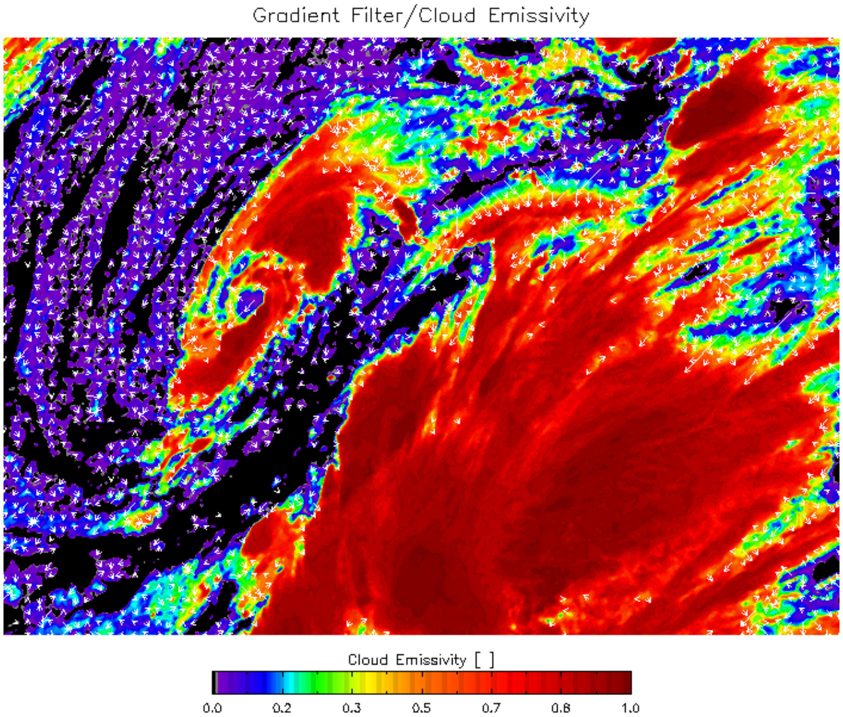

Gradient Filter/Cloud Emissivity

Cloud Emissivity [ ]
0.0
0.2
0.3
0.5
0.7
0.8
1.0

Figure 26: The gradient vector with respect to cloud emissivity at the top of the troposphere is shown overlaid on a false color RGB image (top) and the actual cloud emissivity image itself (bottom). The tail of the arrow indicates the reference pixel location.

While the above was a generalized description of the gradient filter, we next describe the method for calculating the LRC (the gradient vector).

The LRC subroutine (also known as the gradient filter) uses the following inputs

1. The value on which the gradient is being calculated on (Grad_Input)
2. The number of elements in the current segment
3. The number of lines in the current segment
4. LRC Mask for the current segment
5. The minimum allowed input value (Min_Grad)
6. The maximum allowed input value (Max_Grid)
7. The gradient stop value (Grad_Stop)

The input values to the LRC routine are typically either the 11μm troposphere emissivity, $\varepsilon_{stropo}(11\mu m)$, the nadir corrected 11μm troposphere emissivity, $\varepsilon_{stropo, nadir}(11\mu m)$ or the 11μm brightness temperature. A full list of the input values for each algorithm is listed in Table 1. The output for the LRC algorithm is as follows:

1. Array of element indices of the LRCs for the current segment
2. Array of line indices of the LRCs for the current segment

The first thing that is done for a given segment of data is the computation of the yes/no (1/0) LRC Mask. This mask simply states what pixels the LRC will be computed for. For each algorithm, the definition for the LRC mask criteria is defined in table 1.

The LRC routine loops over every line and element, calculating the LRC for each pixel individually. For all valid pixels, the LRC algorithm initially uses information from the surrounding 8 pixels (i.e a 3x3 box centered on the given pixel) to determine the direction of the gradient vector. The number of pixels used is the same for each algorithm. The validity of a given reference pixel (G_{ref}) is determined by the following criteria

1. Does the pixel have a value greater than the minimum allowed value (Min_Grad)?
2. Does the pixel have a value less than the maximum allowed input value (Max_Value)?
3. Is LRC mask is set to “Yes”?

If any of the above statements are false, the LRC algorithm will simply skip over that particular pixel. However, if all three statements are true, then the pixel is considered valid and the algorithm will proceed to the next step.

The next step in the gradient filter is the determination of the initial direction of the gradient. Initially, the gradient test value (G_{test}), which is a local variable, set to a large number (99999) and the direction is set to missing. The gradient (G_{diff}) between the reference pixel (G_{ref}) and the neighboring pixel is calculated. This difference is only calculated if the neighboring pixel is greater than or equal to Min_Grad and less than or equal to Max_Grad. For each direction, if G_{diff} is less than G_{test} , then G_{test} is set to G_{diff}. G_{diff} is calculated for each of the 8 surrounding pixels, and the direction that has the smallest G_{test} is selected as the direction to look for the local radiative center. If the direction is set to missing, then the LRC routine moves to the next pixel in the segment. This can only occur if all the surrounding pixels are either smaller than Grad_Min or greater than Grad_Max.

The directions of the gradient are specified in the following manner:

Table 1. Definition of the directions used in the gradient filter.

Direction #	Y direction	X direction
1	Elem - 1	Line + 0
2	Elem - 1	Line + 1
3	Elem + 0	Line + 1
4	Elem + 1	Line + 1
5	Elem +1	Line + 0
6	Elem +1	Line - 1
7	Elem + 0	Line - 1
8	Elem - 1	Line - 1

One the direction of the gradient has been established, the gradient filter then looks out in the direction for one of six stopping conditions:

1. The test pixel is less than or equal to Min_Grad
2. The test pixel is greater than or equal to Max_Grad
3. The test pixel is greater than or equal to the stop value (Grad_Stop)
4. The test pixel is less than the reference pixel.
5. The gradient filter has reached the maximum number of steps to look out
6. The test pixel is at the edge of the segment

Table 2 shows how the gradient determines the test pixel. For example, for pixel 30,30 of a given segment, if the gradient direction is #3, then the gradient filter tests along (30, 30+n), where n is the current step being tested. Once one of these conditions is met, the line element number is stored as the LRC for the given reference pixel. Originally, the maximum number of steps that could be taken was set to 150. However, a study done by Michael Pavolonis (NOAA/NESDIS) showed that the average number of steps that are needed to find the LRC is less than or equal to 30, as can be seen in figure 2.

5. CRTM

a. Data *description*

Description: Community radiative transfer model
Filename: N/A
Origin: NOAA / NESDIS
Size: N/A
Static/Dynamic: N/A

b. Interpolation *description*

A double linear interpolation is applied in the interpolation of the transmissitance and radiance profile, as well as in the surface emissivity, from four nearest neighbor NWP grid points to the satellite observation point. There is no curvature effect. The weights of the four points are defined by the Latitude / Longitude difference between neighbor NWP grid points and the satellite observation point. The weight is defined with subroutine ValueToGrid_Coord:

NWP forecast data is in a regular grid.

Suppose:
Latitude and Longitude of the four points are:
(Lat1, Lon1), (Lat1, Lon2), (Lat2, Lon1), (Lat2, Lon2)
Satellite observation point is:
(Lat, Lon)

Define
aLat = (Lat – Lat1) / (Lat2 – Lat1)
alon = (Lon – Lon1) / (Lon2 – Lon1)

Then the weights at four points are:
w11 = aLat * aLon
w12 = aLat * (1 – aLon)
w21 = (1 – aLat) * aLon
w22 = (1-aLat) * (1 – aLon)

Also define variable at the four points are:

a11, a12, a21, a22

Then the corresponding interpolated result at satellite observation point (Lat, Lon) should be:

a(Lat, Lon) = (a11*w11 + a12*w12 + a21*w21 + a22*w22) / u

Where,

u = w11 + w12 + w21 + w22

c. CRTM calling procedure in the AIT framework

The NWP GFS pressure, temperature, moisture and ozone profiles start on 101 pressure levels.
They are converted to 100 layers in subroutine Compute_Layer_Properties. The layer temperature between two levels is simply the average of the temperature on the two levels.
layer_temperature(i) = (level_temperature(i) + level_temperature(i+1))/2
While pressure, moisture and ozone are assume to be exponential with height.
hp = (log(p1)-log(p2))/(z1-z2)
p = p1* exp(z*hp)
Where p is layer pressure, moisture or ozone. p1,p2 represent level pressure, moisture or ozone. z is the height of the layer.

CRTM needs to be initialized before calling. This is done in subroutine Initialize_OPTRAN. In this call, you tell CRTM which satellite you will run the model. The sensor name is passed through function call CRTM_Init. The sensor name is used to construct the sensor specific SpcCoeff and TauCoeff filenames containing the necessary coefficient data, i.e. seviri_m08.SpcCoeff.bin and seviri_m08.TauCoeff.bin. The sensor names have to match the coefficient file names. You will allocate the output array, which is RTSolution, for the number of channels of the satellite and the number of profiles. You also allocate memory for the CRTM Options, Atmosphere and RTSoluiton structure. Here we allocate the second RTSolution array for the second CRTM call to calculate derivatives for SST algorithm.

Before you call CRTM forward model, load the 100-layer pressure, temperature, Moisture and ozone profiles and the 101 level pressure profile into the Atmosphere Structure. Set the units for the two absorbers (H2O and O3) to be MASS_MIXING_RATIO_UNITS and VOLUME_MIXING_RATIO_UNITS respectively. Set the Water_Coverage in Surface structure to be 100% in order to get surface emissivity over water. Land surface emissivity will be using SEEBOR.

Also set other variables in Surface data structure, such as wind speed/direction and surface temperature. Use NWP surface temperature for land and coastline, and OISST sea surface temperature for water. Set Sensor_Zenith_Angle and Source_Zenith_Angle in Geometry structure. Call CRTM_Forward with normal NWP profiles to fill RTSolution, then call CRTM_Forward again with moisture profile multiplied by 1.05 to fill RTSolution_SST. The subroutine for this step is Call_OPTRAN.

After calling CRTM forward model, loop through each channel to calculate transmittance from each level to Top of Atmosphere (TOA). What you get from RTSolution is layer optical depth, to get transmittance

```
 Trans_Atm_Clr(1) = 1.0

 Do Level =  2 , TotalLevels
    Layer_OD = RTSolution(ChnCounter, 1)%Layer_Optical_Depth(Level
-1)
    Layer_OD = Layer_OD /
COS(CRTM%Grid%RTM(LonIndex,LatIndex) &
                  %d(Virtual_ZenAngle_Index)%SatZenAng * DTOR)
    Trans_Atm_Clr(Level) = EXP(-1 * Layer_OD) &
                 * Trans_Atm_Clr(Level - 1)
 ENDDO
```

DTOR is degree to radius PI/180.

Radiance and cloud profiles are calculated in Clear_Radiance_Prof

```
 SUBROUTINE Clear_Radiance_Prof(ChnIndex, TempProf, TauProf,
RadProf, &
                     CloudProf)
 B1 = Planck_Rad_Fast(ChnIndex, TempProf(1))
 RadProf(1) = 0.0_SINGLE
 CloudProf(1) = B1*TauProf(1)

 DO LevelIndex=2, NumLevels
    B2 = Planck_Rad_Fast(ChnIndex, TempProf(LevelIndex))
    dtrn = -(TauProf(LevelIndex) - TauProf(LevelIndex-1))
    RadProf(LevelIndex) = RadProf(LevelIndex-1) +
(B1+B2)/2.0_SINGLE * dtrn


    CloudProf(LevelIndex) = RadProf(LevelIndex) +
B2*TauProf(LevelIndex)
    B1 = B2
 END DO
```

Transmittance, radiance and cloud profiles are calculated for both normal CRTM structure and the 2^{nd} CRTM structure for SST.

Call Clear_Radiance_TOA to get TOA clear-sky radiance and brightness temperature.

```
SUBROUTINE Clear_Radiance_TOA(Option, ChnIndex, RadAtm,
TauAtm, SfcTemp, &
                              SfcEmiss, RadClr, BrTemp_Clr, Rad_Down)
IF(Option == 1) THEN
  IF(PRESENT(Rad_Down))THEN
    RadClr = RadAtm + (SfcEmiss * Planck_Rad_Fast(ChnIndex,
SfcTemp) &
         + (1. - SfcEmiss) * Rad_Down) * TauAtm
  ELSE
    RadClr = RadAtm + SfcEmiss * Planck_Rad_Fast(ChnIndex,
SfcTemp) &
             * TauAtm
  ENDIF

  CALL Planck_Temp(ChnIndex, RadClr, BrTemp_Clr)

 ELSE
   RadClr = 0.0
   BrTemp_Clr = 0.0
ENDIF
```

In this subroutine, Rad_Down is optional, depending on if you want to have a reflection part from downward radiance when you calculate the clear-sky radiance. Notice that clear-sky radiance and brightness temperature on NWP grid only calculated for normal CRTM structure not the SST CRTM structure.

Also save the downward radiances from RTSolution and RTSolution_SST to CRTM_RadDown and CRTM_RadDown_SST. Save CRTM calculated surface emissivity to CRTM_SfcEmiss. The above steps are done in subroutine CRTM_OPTRAN